AMERICAN MUSEUM NOVITATES

An Introduction to the Systematics of Small-bodied *Neacomys* (Rodentia: Cricetidae) from Peru with Descriptions of Two New Species

PAMELA SÁNCHEZ-VENDIZÚ,[1, 2] VÍCTOR PACHECO,[1] AND DAN VIVAS-RUIZ[3]

ABSTRACT

The genus *Neacomys* includes 10 recognized species of Neotropical spiny mice in the tribe Oryzomyini. Five species have previously been reported from Peru, but the small-bodied Peruvian taxa remain unrevised. In this report, we present the first systematic and taxonomic revision of small-bodied *Neacomys* populations in Peru and describe two new species based on molecular, morphological, and karyotype data: (1) *Neacomys rosalindae*, sp. nov., from northeastern Peru, is distinguished from congeneric species by, among other differences, short incisive foramina with a wide maxillary portion of the septum, a small subsquamosal fenestra, and a karyotype of $2n = 48$, FN = 50. (2) *Neacomys macedoruizi*, sp. nov., from central Peru, is distinguished by its gray-based ventral fur, large infraorbital foramen, and karyotype of $2n = 28$, FN = 36, with a distinctively large pair of metacentric chromosomes. The results of our molecular analyses suggest that *N. minutus* (as currently recognized) is a species complex comprised of *N. minutus* sensu stricto, *N. macedoruizi*, and a third form that remains to be described. The other species described here, *N. rosalindae*, is the sister taxon to a cluster that includes the *N. minutus* complex plus *N. musseri*. Our data suggest that the upper Amazon River constitutes an important dispersal barrier for species in this genus.

[1] Departamento de Mastozoología, Museo de Historia Natural, Universidad Nacional Mayor de San Marcos, Lima, Peru.
[2] Asociación Grupo RANA, Lima, Peru.
[3] Laboratorio de Biología Molecular, Facultad de Ciencias Biológicas, Universidad Nacional Mayor de San Marcos, Lima, Peru.

INTRODUCTION

Neacomys Thomas, 1900, is a genus of small oryzomine rodents characterized by having eight mammae, grooved spines in their dorsal fur, and typically grizzled yellowish-brown dorsal coloration. Ten species are currently recognized: *N. amoenus* Thomas, 1904; *N. dubosti* Voss et al., 2001; *N. guianae* Thomas, 1905; *N. minutus* Patton et al., 2000; *N. musseri* Patton et al., 2000; *N. paracou* Voss et al., 2001; *N. pictus* Goldman, 1912; *N. spinosus* (Thomas, 1882); *N. tenuipes* Thomas, 1900; and *N. vargasllosai* Hurtado and Pacheco, 2017. Most species of *Neacomys* are Amazonian in distribution, although *N. pictus* occurs only in eastern Panama and *N. tenuipes* occurs in the Colombian Andes and northern Venezuela (Weksler and Bonvicino, 2015).

Recent studies of Aniskin (1994) and Malygin and Rosmiarek (1996) described a new karyotype and morphological characteristics of a potentially new species of *Neacomys* from northeastern Peru, and subsequent molecular analyses of *Neacomys* (Patton et al., 2000; Catzeflis and Tilak, 2009; Hurtado and Pacheco, 2017) have shown that the diversity of species in western Amazonia has been underestimated. Additionally, these studies showed that the small-bodied forms do not comprise a monophyletic group, consisting of at least seven highly divergent taxa, of which three remain undescribed. One of these unnamed forms was informally called *N.* "sp. (clade 3)" by Patton et al. (2000) and occurs in northeastern Peru and eastern Ecuador. Patton et al. (2000) suggested that their "clade 3" might be the same as the undescribed species represented by Aniskin's (1994) and Malygin and Rosmiarek's (1996) specimens. However, no further studies have been carried out to confirm the taxonomic status of this still-undescribed form. Therefore, only two valid small-bodied species, *N. minutus* and *N. musseri*, are currently recognized from Peru (Weksler and Bonvicino, 2015; Hurtado and Pacheco, 2017).

Neacomys minutus and *N. musseri* were originally described on the basis of morphological and molecular data from specimens collected south of the Amazon River, but Tirira (2007) subsequently reported *N.* "cf. *minutus*" from eastern Ecuador, and Hurtado and Pacheco (2017) reported *N. minutus* from the National Reserve Pucacuro in northeastern Peru (north of the Amazon). Nevertheless, based on the molecular results of Patton et al. (2000), Tirira's and Hurtado and Pacheco's specimens are more likely to represent *N.* "sp. (clade 3)" instead of *N. minutus*. Moreover, Weksler and Bonvicino (2015) suggested that the molecular and morphometric differences between the "upriver" and "downriver" clades of *N. minutus* discussed by Patton et al. (2000) are evidence that these clades are distinct species. It therefore seems probable that *N. minutus* is a species complex. This inference is reinforced by our recent discovery of a new central Peruvian population of small-bodied *Neacomys* similar to, but apparently distinct from, *N. minutus*. Herein we provide morphological, karyotypic, and molecular analyses of small-bodied *Neacomys* from Peru to clarify their systematic and taxonomic status.

MATERIALS AND METHODS

Specimens Examined

We examined a total of 125 specimens of small-bodied *Neacomys* housed in the following institutions: AMNH, American Museum of Natural History, New York; FMNH, Field Museum

of Natural History, Chicago; MUSA, Museo de la Universidad Nacional de San Agustín, Arequipa; MUSM, Museo de Historia Natural de la Universidad Nacional Mayor de San Marcos, Lima; MVZ, Museum of Vertebrate Zoology, University of California, Berkeley; and USNM, National Museum of Natural History, Smithsonian Institution, Washington, D.C. This morphological material is listed in appendix 1.

CYTOGENETIC ANALYSIS

To obtain chromosomal samples we followed the methods described by Ford and Hamerton (1956), Patton (1967), Baker and Qumsiyeh (1988), and Baker et al. (2003) with some modifications. The work was performed at the laboratory of cytogenetic and molecular systematics of the Universidad Nacional Mayor de San Marcos, Lima (MUSM). Live specimens were weighed and injected intraperitoneally with colchicine (0.1 ml/10 g). After 40 minutes, the animals were euthanized using ketamine (Halatal®KT, 10% ketamine) and measured for external dimensions (total length, tail length, hindfoot length, and ear length). The marrow cavity of the femur was flushed with warm (37° C) hypotonic solution (0.075 M of KCl). The resulting cell suspension was incubated at 37° C for 20 min in a centrifuge tube, centrifuged until a good pellet was obtained, and the supernatant was decanted. Carnoy's solution (3:1 ethanol:acetic acid) was then added to resuspend the pellet and fix the cell suspension. In the laboratory, the sample was rewashed with Carnoy's solution until the supernatant was clean. The slides were prepared and stained with Giemsa (2%). The slides were reviewed using a microscope with a built-in 5 MP Leica D750 camera. To construct the karyotype, 100 metaphase plates were revised for each individual. We determined the diploid number ($2n$) and the fundamental number (FN) for each species. The classification of chromosomes was based on Levan et al. (1964) and Patton (1967). Slides are housed in the MUSM.

MOLECULAR ANALYSIS

We isolated DNA from small fragments of muscle tissues following the specific protocols of the DNA genomic isolation kit (GeneOn "Vivantis" GF-TD-100: 100 preps and THERMO: 50 preps). Isolated DNA was preserved at -20° C and used to amplify a fragment of 801 bp of the mitochondrial gene cytochrome *b* (cyt-*b*) by the polymerase chain reaction (PCR) with primers MVZ 005 and MVZ 016 (Smith and Patton, 1993). Amplicons were sequenced by Macrogen, Inc (Seoul, South Korea). Sequence editing was performed using CodonCode Aligner v. 6.0.2. Sequences were translated to protein using the ExPASy web portal (http://web.expasy.org/translate/) to avoid artificial codons and to verify the correct edition of sequences. New sequences were uploaded to Genbank.

Phylogenetic analyses were performed using cyt-*b* sequences previously reported by Patton et al. (2000), Catzeflis and Tilak (2009), and Hurtado and Pacheco (2017), together with new sequences obtained in this study. In total, we analyzed sequence data from 108 individuals representing nine named species and the three undescribed forms that Patton et al. (2000) called "clade 3," "clade 6," and "clade 7." Our selected outgroups included sigmodontine species in the tribes Akodontini (*Akodon mollis*), Oryzomyini (*Oligoryzomys microtis, Oecomys bicolor, Micro-*

ryzomys minutus), and Thomasomyini (*Thomasomys daphne, Rhipidomys macconnelli*). All the sequences we analyzed (including ingroup and outgroup terminals) are listed in appendix 2.

Sequence alignment was executed with MEGA v. 7.0.14 using Clustal W (Thompson et al., 1997) with a final length of 801 bp. The best nucleotide substitution model was evaluated using jModelTest v. 2.1.7 (Darriba et al., 2012) with the Akaike Information Criterion (AIC). The best-fitting substitution model was GTR+I+G, which was implemented a priori in the Bayesian inference (BI) and maximum-likelihood (ML) phylogenetic analyses.

Bayesian inference was executed with Bayesian Analysis of Phylogeny (MrBayes v. 3.2.6 × 64; Ronquist and Huelsenbeck, 2003) consisting of two independents runs. Each run had 20 million generations with sampling at every 1000 generations. The standard deviation was 0.003 (less than 0.01) and the estimated sample size was 12298 (over 100), which indicate convergence of the analysis. The first 25% of samples were discarded, and the posterior probabilities at nodes with values equal to or greater than 95% were considered significant. ML analysis was carried out using the randomized accelerated maximum-likelihood algorithm (RAxML v 8.2.7; Stamatakis, 2014). Nodal support was computed using 1000 bootstrap replicates. Bootstrap values >90% were considered strong support (Hillis and Bull, 1993; Catzeflis and Tilak, 2009). Phylogenetic trees were edited in FigTree v. 1.4.2 and Inkscape 0.9. Uncorrected genetic distances (*p*-distances) were calculated with MEGA v. 7.0.14.

Morphological Terminology and Morphometric Analysis

We followed the terminology and measurements of external and craniodental features described by Patton et al. (2000) and Voss et al. (2001). Characters of the molar dentition follow Reig (1977). Age classification of the examined specimens is based on molar toothwear criteria described by Voss (1991). The following external measurements were recorded (to nearest millimeter, mm) from specimen labels:

Total length (TL): measured from the tip of nose to tip of the terminal tail vertebra

Tail length (TaL): measured from dorsal flexure at the base of the tail to the tip of the last vertebra

Hindfoot length (HL): measured from proximal margin of the calcaneus to the tip of longest claw

Ear length (EL): measured from notch to top of the pinna

Head and body length (HBL) was subsequently calculated as the difference between total length and the tail length (HBL = TL – TaL)

Twenty-four measurements of the skull and dentition were taken with digital calipers and recorded to the nearest 0.01 mm:

Condylo-incisive length (CIL): measured from the anterior margins of the upper incisors to the posterior margins of the occipital condyles

Zygomatic breadth (ZB): greatest breath across the zygomatic arches

Braincase breadth (BB): greatest breath above and slightly behind the squamosal zygomatic processes

Interorbital constriction (IOC): least distance across the roof of the skull between the orbits

Rostral length (RL): from the tip of one nasal bone to the posterior margin of the zygomatic notch on the same side

Nasal length (NL): the greatest anterior-posterior dimension of one nasal bone

Rostral width (RW-1): measurement taken across the outside margins of the nasolacrimal capsules

Rostral width 2 (RW-2): measurement taken at the premaxilla-maxilla suture

Orbital length (OL): taken from the most anterior to the most posterior margins of the orbit

Diastema length (DL): distance from the posterior face of the upper incisors to the anterior edge of M1 on the same side

Maxillary toothrow length (MTRL): crown length of the maxillary toothrow

Incisive foramen length (IFL): greatest length of one incisive foramina

Palatal length (PL): distance from the posterior face of an upper incisor to the anterior margin of the mesopterygid fossa on the same side

Alveolar width (AW): outside distance across the alveoli of the left and right first upper molars

Occipital condyle breath (OCB): outside distance across the occipital condyles

Mastoid breadth (MB): greatest width across the mastoid processes

Basioccipital length (BOL): distance from the anterior margin of the foramen magnum to the basioccipital-basisphenoid suture

Mesopterygoid fossa length (MPFL): midline distance from the anterior margin of the meso-pterygoid fossa to the posterior tips of the hamular processes of the pterygoids

Mesopterygoid fossa wide (MPFW): maximal width taken at the suture between the palatine and pterygoid bones.

Zygomatic plate length (ZPL): measurement taken at midheight from the anterior to the posterior margins of the zygomatic plate

Cranial depth (CD): measured by placing the skull on a glass slide, measuring the distance from the bottom of the slide to the top of the cranial vault, and subtracting the thickness of the slide

Breadth of incisive foramen (BIF): greatest transverse dimension across both incisive foramina

Breadth of the palatal bridge (BPB): measurement taken between the protocones of the right and left first maxillary molars

Breadth of M1 (BM1): greatest crown breadth of the first maxillary molar

Variables were assessed for univariate normality with Shapiro-Wilk tests. Sexual dimorphism was tested with a multivariate analysis of variance (MANOVA) based on the largest available population sample from northeastern Peru ($N_{females} = 31$, $N_{males} = 36$), but no significant differences were found ($\lambda = 0.388$, $p > 0.05$). Therefore, the sexes were combined for subsequent morphometric analyses. We did not analyze morphometric variation among age classes

because of the unbalanced numbers of specimens among toothwear categories ($N_{age\,II} = 8$, $N_{age\,III} = 40$, $N_{age\,IV} = 18$, $N_{age\,V} = 1$). Statistical analysis for geographic variation was performed with specimens of age classes III, IV, and V, all of which were considered adults (Voss, 1991; Rengifo and Pacheco, 2015). Principal components analyses (PCA) and MANOVA were performed to evaluate differences between closely related species as determined by phylogenetic analysis. All analyses and graphics were executed in SPSS v 23 and SigmaPlot v10.

RESULTS

Neacomys macedoruizi, new species

Figures 1, 2, 3C, 4C, 5A, 6D

HOLOTYPE: A young adult male (age class III) specimen housed in the Museo de Historia Natural de la Universidad Nacional Mayor de San Marcos (MUSM 45053), collected by P.S.-V. on December 8, 2015 (original field number PSV 021). The holotype is preserved in fluid, with the skull extracted and cleaned.

PARATYPES: We refer three other examined specimens, all consisting of fluid-preserved bodies with extracted and cleaned skulls: MUSM 45054 (male, age II), MUSA 19680 (male, age III), MUSA 19692 (female, age V).

TYPE LOCALITY: Peru, Department of Huánuco, Province of Leoncio Prado, Tingo María National Park, Puesto de Control 3 de Mayo; 9°24′25.71′′S, 76°0′13.39′′W, 1129 m

DIAGNOSIS: A small species of *Neacomys* distinguished from other congeneric taxa by its bicolored ventral fur (the individual hairs are white distally with gray bases); large infraorbital foramina; relatively long rostrum with nasal bones expanded anteriorly; relatively large nasolacrimal capsules; well-developed, straight, and posteriorly strongly divergent supraorbital ridges; large subsquamosal fenestra (almost half the size of the postglenoid foramen on each side of the skull); long subrectangular incisive foramina that extend posteriorly close to M1; narrow maxillary portion of the septum of incisive foramina; large posterolateral palatal pits (one on each side, each with small foramina inside); long and narrow bony eustachian tubes, mostly in contact with the basisphenoid bone; and anterocone with a deep anteromedian flexus.

MORPHOLOGICAL DESCRIPTION: The dorsal pelage of *Neacomys macedoruizi* is typically orange and sparsely streaked with black, especially on the middle back and the rump, and becoming paler (yellowish orange) along the sides. In the youngest specimen we examined (MUSM 45054), the color of the sides is darker (more orange). All specimens exhibit a narrow orange lateral line that separates the dorsal and ventral pelage. The ventral fur is superficially white from chin to anus, but the individual hairs are grayish basally, usually for about 10% of their length. The fur on the inner surfaces of the arms and legs have hairs that are gray for about 30% of their length. The genal, superciliary, and mystacial vibrissae are long, extending behind the pinnae when laid back alongside the head. The tail is slightly longer than the head and body, strongly bicolored (dark above, pale below) on its proximal half but unicolored (all-dark) distally; there are 20 or 21 caudal scale rows per centimeter, and a small tuft of hair is

FIGURE 1. *Neacomys macedoruizi* (MUSA 19692). Notice the bicolored ventral fur (image at upper right). Photo by Alexander Pari Chipana.

present at the tip of the tail. The hind feet are small and narrow with six fleshy, rounded plantar pads; the dorsal pelage of the hind feet is white with a pale-brown spot over the metatarsals in some specimens. The digits are long and slender with white ungual tufts that exceed the claws in length, except on the first digit, which has a shorter tuft. The claw of pedal digit I only reaches the base of the first phalange of digit II, whereas the claw of digit V reaches the end of the first phalange of digit IV.

The skull is robust with a convex profile and appears teardrop shaped in dorsal view (fig. 2). The nasal bones are expanded anteriorly, appearing somewhat spatulate. The zygomatic notch is comparatively large and deep. The lacrimals are small and almost rounded. The supraorbital ridges are well developed, and the interorbital region is straight and strongly divergent posteriorly. The carotid circulation conforms to pattern 1 (Voss, 1988: fig. 18A, B) with a distinct stapedial foramen, squamosal-alisphenoid groove, and sphenofrontal foramen. The sphenopalatine foramen is large. The subsquamosal fenestra and the postglenoid foramen are large apertures on each side of the skull, and the hamular process of the squamosal that separates them is long. The paroccipital processes are robust, slightly curved anteriorly and well separated from the auditory bullae (fig. 3C). The incisive foramina are long, narrow, and almost rectangular in outline; they

extend posteriorly almost, but not quite, to the anterior alveolus of M1. The maxillary portion of the septum is narrow (fig. 4C). Only one deep, ovoid, and well-defined posterolateral palatal pit is present on each side, approximately level with the posterior alveolus of M3. The mesopterygoid fossa is narrow with a biconcave anterior margin, and it does not reach the posterior alveolus of M3. The lateral margin of the pterygoid plate is distinctly angular. The oval foramen is large. The auditory bullae are flask shaped, with long and narrow bony eustachian tubes. The carotid canal has a large aperture. In frontal view (fig. 5A), the infraorbital foramen is widely open, and the zygomatic plate is robust and slightly inclined outward.

The maxillary toothrow is short in relation to the diastema; the first upper molars are somewhat rectangular in outline. On M1, the anterocone is divided into distinct anterolabial and anterolingual conules by a well-developed anteromedian flexus; the anteroloph is always fused with the anterolabial conule, so the anteroflexus is not distinguishable (fig. 6D); the mesoloph is straight, slender, and extends to the labial cingulum; the posteroloph is short, slim, and usually fused with the metacone on more worn teeth; the paraflexus and mesoflexus are long and deep; the metaflexus is long and convex; the posteroflexus is short and conspicuous only on unworn teeth, whereas the protoflexus and hypoflexus are very distinct. M2 is more or less square in occlusal outline and exhibits a distinct internal fossette; the anteroloph is long and very slim; the mesoloph is slim, almost straight, and reaches the labial cingulum; the posteroloph is very short and usually fused with the metacone on worn teeth; the paraflexus is well developed and long; the mesoflexus is short, whereas the metaflexus is long and deep. M3 is small, almost half the size of M2, and triangular in occlusal outline; this tooth exhibits a very short anteroloph, paraflexus, and mesoflexus, but other enameled structures are not evident.

On the mandible, the m1 anteroconid lacks an anteromedian flexid; the anterolophid is fused with the anteroconid; the mesolophid is usually not evident because it appears to be fused with the entoconid, and the posterolophid is also fused with the entoconid; the metaflexid is short; the mesoflexid is conspicuous; the entoflexid is absent or reduced to a small fossetid, whereas the protoflexid and hypoflexid are well developed. On m2 the anterolabial cingulum is very short; the protoflexid is short but distinct; the hypoflexid is long and deep; the mesoflexid is long; the mesolophid is usually fused with the entoconid; and the posterolophid is wide. On m3 the protoconid, metaconid, and hypoconid are well developed; the protoflexid is very short or indistinct; the hypoflexid is well developed; the mesoflexid is noticed but only as small fossetid; the posteroflexid is absent or very small, visible as a small fossetid; and the mesolophid and entoconid are indistinct and apparently fused with the metaconid and posterolophid.

KARYOTYPES: Conventional cytogenetic (Giemsa-stained) preparations of two specimens of *Neacomys macedoruizi* (MUSM 45053 and 45054, both males) revealed the lowest diploid and fundamental numbers known for the genus ($2n = 28$, FN = 36). The karyotype includes five pairs of metacentric autosomes (one large, one medium, and three small) and eight pairs of acrocentric autosomes (one large and seven small); the X chromosome is a medium-size submetacentric, and the Y chromosome is a small acrocentric (fig. 7C).

MEASUREMENTS OF HOLOTYPE: HBL, 76; TaL, 71; HFL, 22; EL: 14.5; CIL, 18.66; ZB, 10.71; BB, 10.42; IOC, 4.16; RL, 7.2; NL, 7.9; RW-1, 4.51; RW-2, 2.72; OL, 7.11; DL, 5.34; MTRL, 2.57;

FIGURE 2. Dorsal, ventral, and lateral views of the cranium and mandible of *Neacomys macedoruizi* (MUSM 45053, holotype).
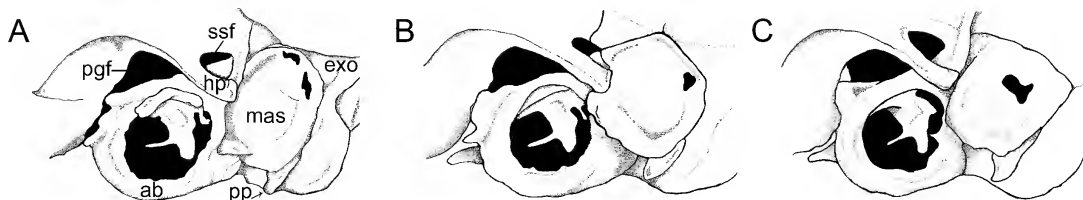
FIGURE 3. Lateral view of left auditory region illustrating variation in size and morphology of the subsquamosal fenestra and the distance between the paraoccipital process and the auditory bulla. **A,** *Neacomys minutus* (INPA 2689, taken from Patton et al. [2000]). **B,** *Neacomys rosalindae* (MUSM 44963). **C,** *Neacomys macedoruizi* (MUSM 45053). Abbreviations: **ab,** auditory bulla; **exo,** exoccipital; **hp,** hamular process of squamosal; **mas,** mastoid; **pgf,** postglenoid foramen; **pp,** paraoccipital process; **ssf,** subsquamosal fenestra.

IFL, 3.12; PL, 8.25; AW, 3.69; OCB, 5.38; MB, 9.70; BOL, 3.00; MPFL, 2.69; MPFW, 1.48; ZPL, 1.88; CD, 7.69; BIF, 1.52; BPB, 2.21; BM1, 2.74. Measurements of additional specimens are provided in table 1.

DISTRIBUTION AND SYMPATRY: *Neacomys macedoruizi* is currently known only from the Tingo María National Park (province of Leoncio Prado, department of Huánuco, Peru). It was collected near the Puesto de Control 3 de Mayo on the road that leads to the "Salto del Ángel" waterfall. The local habitat corresponds to primary premontane rainforest and is characterized by medium-size trees (15–20 m high) and sparse understory vegetation growing on very steep terrain. The specimens were collected near water sources, close to the waterfall "Salto del Ángel" and adjacent to small ravines. At the same locality, we also collected a larger congeneric species, *N. amoenus.*

COMPARISONS: Based on size and morphology *Neacomys macedoruizi* could only be confused with two previously described western Amazonian species, *N. musseri* and *N. minutus* (table 2). In external comparisons with *N. musseri*, the dorsal fur of *N. macedoruizi* is less streaked with black, especially on the rump; the ventral fur is gray based (versus pure white in *N. musseri*); and the tail is strongly bicolored basally with 20–21 scale rows per cm (versus weakly bicolored with only 16 scale rows per cm on average in *N. musseri*; Patton et al., 2000). In cranial comparisons, *N. macedoruizi* has a primitive carotid circulation pattern (versus pattern 2 [Voss, 1988] in *N. musseri*), larger and deeper zygomatic notches, almost straight (versus strongly convex) lateral margins of the incisive foramina, flask-shaped (versus more globular) auditory bullae with longer (versus shorter and wider) bony eustachian tubes, and a seldom-distinct (versus well-developed) M1 anteroloph.

Neacomys macedoruizi is morphologically more similar to *N. minutus* but differs from that species by its gray-based ventral fur (the ventral fur is pure white in *N. minutus*), large (versus small) nasolacrimal capsules, wider infraorbital foramen, deeper zygomatic notches, incisive foramina with almost straight (versus convex) lateral margins, a deep (versus shallow) posterolateral palatal pit that is much closer to the posterior margin of the M3 alveolus on each side; and a deep (versus weakly developed) anteromedian flexus on M1.

Neacomys macedoruizi is easily distinguished from its sympatric congener *N. amoenus* by its smaller size (e.g., HBL <80 mm versus HBL >80 mm), more slender and smaller hind feet

FIGURE 4. Ventral views of crania illustrating variation in shape, size, and/or position of the incisive foramina, foraminal septum, nasolacrimal capsules, posteropalatal pits, and molar toothrows. **A**, *Neacomys minutus* (from Patton et al. 2000); **B**, *Neacomys rosalindae* (MUSM 44963); **C**, *Neacomys macedoruizi* (MUSM 45053). Abbreviations: **if**, incisive foramina; **M1**, upper first molar; **nc**, nasolacrimal capsules; **ppp**, posteropalatal pits; **spt**, septum. Scale bar = 5 mm

(HF <22 mm versus HF >22 mm), smaller caudal scales (20–21 scale rows per cm versus 14–16 scale rows per cm), shorter maxillary toothrow (MTRL <2.75 mm versus MTRL >3.00 mm), subrectangular (versus teardrop-shaped) incisive foramina, and well-developed (versus absent or weakly developed) anteromedian flexus on M1.

REMARKS: *Neacomys macedoruizi* is the only species of the *N. minutus* complex that occurs in tropical premontane forest (the others inhabit tropical lowland forest) and is the fourth species that occurs at more than 1000 m after *N. spinosus*, *N. vargasllosai*, and *Neacomys* sp. (Patterson et al., 2006), although the last taxon needs to be revised to verify its affinities with the species of small-bodied *Neacomys*.

ETYMOLOGY: The species is named in honor of Hernando de Macedo Ruiz (fig. 8), curator of the collections of the former "Sección de Aves y Mamíferos" and erstwhile director of MUSM, who worked industriously to promote scientific research in Peru. Among his many achievements were the creation of the journal "Folia Biologica Andina," the establishment of the "Estación Altoandina de Biología," the rediscovery of the monkey *Lagothrix flavicauda*, and the enduring commitment he showed to the improvement of the Museo de Historia Natural (Lima, Peru).

Neacomys rosalindae, new species

Figures 3B, 4B, 5B, 6B, 6C, 9–11

Neacomys tenuipes: Lawrence, 1941: 425; part (misidentified specimens from Ecuador and Peru), not *tenuipes* Thomas, 1900.

Neacomys "sp. (Clade 3)": Patton et al., 2000: 244.

Neacomys "cf. *minutus*": Tirira, 2007: 172.

Neacomys "sp. nov.": Hice and Velazco, 2012: 51.

Neacomys minutus: Hurtado and Pacheco, 2017: 34; part (misidentified specimens from Peru), not *minutus* Patton, da Silva, and Malcolm, 2000.

TABLE 1. Mean, standard deviation, range (in parenthesis) and sample size of external and cranial measurements (in millimeters) of four small-bodied species of *Neacomys*.

	N. rosalindae	N. macedoruizi	N. minutus[a]	N. tenuipes[b]
HBL	75 ± 7 (62–99) 52	74 ± 8 (65–80) 3	71.19 ± 5 (65–79) 16	83 ± 6 (72–97) 33
TaL	77 ± 6 (61.5–87) 46	80 ± 5 (75–85) 3	77.07 ± 5 (70–84) 15	96 ± 8 (74–108) 29
HL	19.85 ± 1 (17–23) 53	19.83 ± 2 (18.5–22) 3	21.15 ± 2 (19–28) 17	22 ±1 (20–24) 34
EL	13.72 ± 2 (11–20) 52	14 ± 1 (13.5–14.5) 3	12.29 ± 1 (10–13) 17	15 ± 2 (12–18) 33
CIL	18.16 ± 0.56 (16.84–19.52) 61	18.48 ± 1.00 (17.40–19.37) 3	17.82 ± 0.49 (16.84–18.74) 21	19.0 ± 0.6 (17.80–20.20) 39
ZB	10.67 ± 0.39 (9.80–11.53) 61	10.71 ± 0.69 (10.22–11.20) 3	10.71 ± 0.30 (10.20–11.67) 21	—
BB	10.09 ± 0.30 (9.19– 10.69) 61	10.35 ± 0.14 (10.18–10.44) 3	10.11 ± 0.29 (9.46–10.73) 21	10.4 ± 0.2 (9.80–10.80) 38
IOC	4.16 ± 0.22 (3.65–4.61) 62	4.11 ± 0.06 (4.04–4.16) 3	4.18 ± 0.16 (3.92–4.50) 21	4.40 ± 0.2 (4.20–4.80) 40
RL	6.61 ± 0.29 (5.99–7.39) 59	6.93 ± 0.56 (6.28–7.30) 3	6.92 ± 0.33 (6.36–7.57) 21	7.0 ± 0.3 (6.40–7.60) 39
NL	8.07 ± 0.35 (6.93–8.85) 59	8.17 ± 0.79 (7.56–9.06) 3	7.76 ± 0.36 (7.16–8.46) 21	—
RW-1	3.97 ± 0.21 (3.44–4.5) 59	4.37 ± 0.25 (4.08–4.52) 3	3.98 ± 0.15 (3.60–4.19) 21	—
RW-2	2.78 ± 0.28 (2.24–3.3) 61	2.88 ± 0.14 (2.72–2.99) 3	3.06 ± 0.14 (2.74–3.28) 21	—
OL	7.00 ± 0.25 (6.49–7.68) 62	6.95 ± 0.35 (6.55–7.18) 3	6.93 ± 0.23 (6.60–7.44) 21	—
DL	5.20 ± 0.25 (4.63–5.97) 62	5.23 ± 0.35 (4.83–5.51) 3	5.13 ± 0.17 (4.80–5.44) 21	5.5 ± 0.3 (4.90–5.90) 40
MTRL	2.61 ± 0.09 (2.37–2.79) 62	2.58 ± 0.02 (2.57–2.61) 3	2.60 ± 0.09 (2.42–2.75) 21	2.8 ± 0.1 (2.70–3.0) 40
IFL	2.83 ± 0.23 (1.85–3.47) 62	3.02 ± 0.1 (2.92–3.12) 3	2.91 ± 0.13 (2.64–3.19) 21	3.1 ± 0.2 (2.50–3.50) 39
PL	8.13 ± 0.30 (7.46–8.78) 61	8.26 ± 0.43 (7.84–8.70) 3	8.04 ± 0.25 (7.64–8.68) 21	—
AW	3.81 ± 0.17 (3.45–4.11) 62	3.75 ± 0.17 (3.62–3.94) 3	4.00 ± 0.18 (3.56–4.27) 21	—
OCB	5.12 ± 0.17 (4.73–5.49) 60	5.30 ± 0.10 (5.19–5.38) 3	5.02 ± 0.28 (4.74–5.77) 21	—
MB	9.34 ± 0.25 (8.87–9.93) 61	9.51 ± 0.46 (8.98–9.84) 3	8.95 ± 0.26 (8.54–9.71) 21	—
BOL	2.87 ± 0.17 (2.39–3.32) 60	3.07 ± 0.21 (2.90–3.30) 3	2.83 ± 0.18 (2.42–3.29) 21	—
MPFL	2.74 ± 0.20 (2.42–3.22) 47	2.59 ± 0.22 (2.34–2.74) 3	2.63 ± 0.17 (2.29–3.00) 21	—
MPFW	1.52 ± 0.13 (1.23–1.75) 59	1.51 ± 0.09 (1.44–1.62) 3	1.72 ± 0.11 (1.47–1.95) 21	—
ZPL	1.79 ± 0.13 (1.43–2.10) 62	1.83 ± 0.07 (1.75–1.88) 3	1.83 ± 0.09 (1.68–2.03) 21	1.9 ± 0.1 (1.60–2.20) 40
CD	7.81 ± 0.22 (7.3–8.45) 61	7.64 ± 0.06 (7.57–7.69) 3	7.42 ± 0.18 (7.09–7.74) 21	—
BIF	1.39 ± 0.09 (1.21–1.60) 62	1.57 ± 0.06 (1.52–1.64) 3	—	—
BPB	2.35 ± 0.17 (1.92–2.75) 61	2.24 ± 0.23 (2.03–2.48) 3	—	2.3 ± 0.1 (2.1–2.7) 39
BM1	0.81 ± 0.07 (0.72–0.90) 62	0.77 ± 0.03 (0.74–0.80) 3	—	—

[a] Measurements provided by J.L. Patton.
[b] Measurements provided by R.S. Voss.

TABLE 2. Morphological and karyotypic comparisons among small-bodied species of *Neacomys* from western Amazonia.

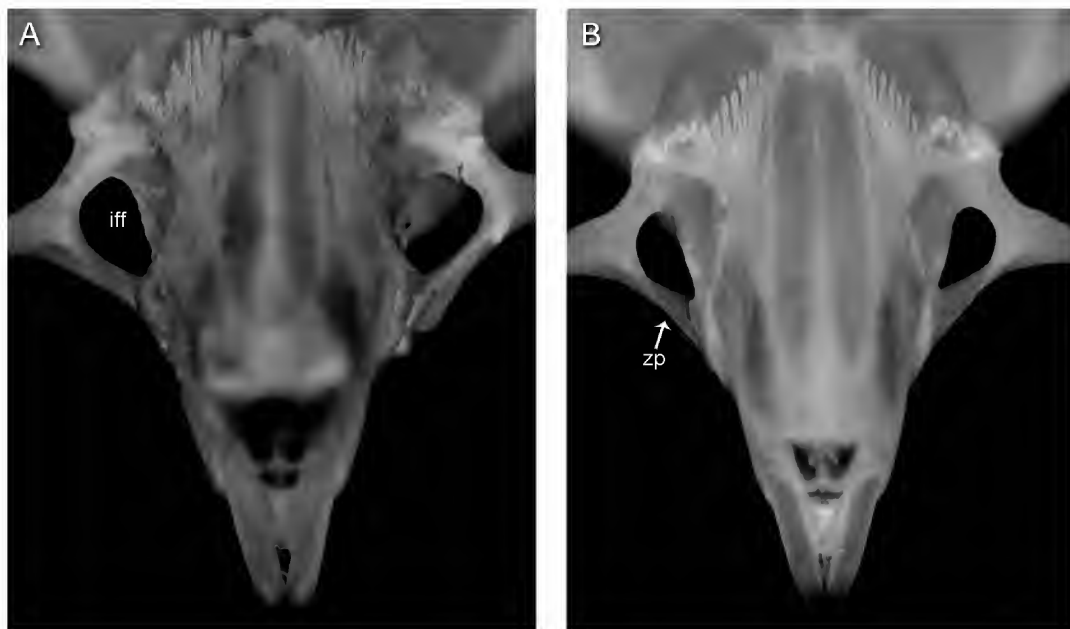| Characters	Neacomys rosalindae	Neacomys macedoruizi	Neacomys minutus	Neacomys tenuipes
Tail length	slightly longer than HB	slightly longer than HB	slightly longer than HB	distinctly longer than HB
Tail coloration	mostly unicolored or incipiently bicolored only at the base	mostly bicolored	mostly bicolored	sharply bicolored
Ventral fur	completely white or slightly buffy.	gray-based white	completely white	white to pale orange
Infraorbital foramen	marrow opening	large opening	narrow opening	narrow opening
Rostrum	short	large	large	large
Nasal bones	narrow anteriorly	expanded anteriorly	—	narrow anteriorly
Nasolacrimal capsule	small	large	small	large
Zygomatic notch	short and shallow	large and slightly deeper	short and shallow	short and shallow
Supraorbital ridges	slightly curved backward	straight and strongly divergent posteriorly	straight and strongly divergent posteriorly	weakly divergent posteriorly
Incisive foramina	short and wide, subrectangular	long and narrow, subrectangular	long and narrow, teardrop shaped	long and wide, teardrop shaped
Septum of incisive foramina	maxillary part wider	maxillary part narrow	maxillary part narrow	maxillary part narrow
Posterolateral palatal pit(s)	usually more than one small pit on each side	one large deep pit on each side	one small pit on each side	more than one large but shallow pit on each side
M1 anterocone	broad and rounded, weakly divided by an anteromedian flexus	narrow and relatively flat, strongly divided by an anteromedian flexus	broad, relatively flat, weakly divided by an anteromedian flexus	broad, rounded or relatively flat; strongly divided by an anteromedian flexus
M1 anteroloph	fused	fused	distinct	distinct
Paraoccipital process	small and closer to auditory bulla	slightly larger and separated from auditory bulla	small and separated from auditory bulla	—
Subsquamosal fenestra	small	conspicuously large	large	large
Sphenopalatine foramen	small	notably large	small	small
Karyotype	$2n = 48$, FN = 50	$2n = 28$, FN = 36	$2n = 35\text{-}36$, FN=40	$2n = 56$

FIGURE 5. Frontal view of rostrum illustrating the size of the infraorbital foramen and the morphology of the zygomatic plate. **A,** *Neacomys macedoruizi* (MUSM 45053). **B,** *Neacomys rosalindae* (MUSM 44971). Abbreviations: **iff,** infraorbital foramen; **zp,** zygomatic plate.

HOLOTYPE: An adult male (age class IV) specimen housed in the Museo de Historia Natural de la Universidad Nacional Mayor de San Marcos (MUSM 44963) collected by Katherine Pino (original field number KPB 1600) on September 19, 2015. The holotype is preserved as skin, skull, and fluid-preserved carcass.

PARATYPES: Thirteen male specimens (MUSM 33873, 33874, 33875, 33892, 33895, 33935, 44963, 44965, 44967, 44968, 44970, 44971, and 44973) and 12 females (MUSM 30350, 33889, 33894, 33896–33898, 33934, 37678, 44962, 44964, 44966, and 44969) preserved as skins, skulls, fluid-preserved carcasses, and skeletons.

TYPE LOCALITY: Peru: Department of Loreto, Province of Maynas, District of San Juan Bautista, Caserio Llanchama; 3°52′18.41″S, 73°23′46.46″W, 122 m above sea level.

DIAGNOSIS: A small species of the genus *Neacomys* characterized by a delicate skull with a wide braincase; well-developed supraorbital ridges that are slightly curved as their lateral margins diverge posteriorly; short and subrectangular incisive foramina with a wider septum than in most other congeneric forms; a small subsquamosal fenestra (much less than half the size of the postglenoid foramen on each side), a short, stout hamular process of the squamosal; a semicircular postglenoid foramen; small, shallow posterolateral palatal pits; and a wide paraoccipital process that is closely approximated to each auditory bulla.

MORPHOLOGICAL DESCRIPTION: The dorsal pelage of *Neacomys rosalindae* is typically deep orange streaked with black, which is more concentrated on the middle back and the rump (figs. 9, 10). The flanks are pale yellow, sometimes with a narrow orange lateral line that clearly separates the dorsal and ventral pelage. The ventral fur is pure white from chin to anus

as well as along the inner surfaces of the arms and legs. The genal, superciliary, and mystacial vibrissae are long and extend behind the pinnae when laid back alongside the head. The tail is slightly longer than the combined length of head and body, sharply or indistinctly bicolored, with 17–24 caudal scales rows per centimeter, and sometimes has a small tuft of hairs at the tip. The hind feet are small and narrow with five or six fleshy plantar pads (the hypothenar pad is reduced or absent). The dorsal pelage of the hind feet is white, usually with a more or less distinct spot of dark brown over the metatarsals. The toes are long and slender, with conspicuous white ungual tufts that are longer than the claws (except dI, which has a short, sparse ungual tuft). The outer digits are short, with the claw of digit I extending only to the base of the first phalange of digit II and the claw of digit V extending just halfway along the first phalange of digit IV.

FIGURE 6. Upper right toothrows illustrating a poorly developed anteromedian flexus on the anterocone of the first upper molar (M1) in *Neacomys minutus* (**A,** picture taken from Patton et al., 2000) and *Neacomys rosalindae* (**B,** MUSM 33894 and **C,** MUSM 44971), but a deep anteromedian flexus on M1 in *Neacomys macedoruizi* (**D,** MUSM 45053). A small internal fossette of the anterocone is present only in *N. rosalindae.*

The skull (fig. 11) is delicate with a wide braincase that appears strikingly globose in dorsal view. The nasal bones are straight, without any conspicuous anterior expansion. The zygomatic notch is shallow. The lacrimals are usually conspicuous and rounded. The supraorbital ridges are well developed, and the interorbital region has lateral margins that appear slightly curved as they smoothly diverge posteriorly. The primitive carotid circulation (pattern I) is indicated by a conspicuous stapedial foramen, a squamosal-alisphenoid groove, and a sphenofrontal foramen on each side. The sphenopalatine foramen is small. The subsquamosal fenestra is small, but in one young specimen (age class II, MUSM 45725) it is somewhat larger than in other conspecifics. The postglenoid foramen is large and semicircular. The hamular process of the squamosal is usually short and proportionately stout. The paraoccipital process is small, robust and close to the auditory bulla (fig. 3B). The incisive foramina are short and subrectangular in outline, with more or less straight lateral margins (in some specimens the lateral margins are slightly concave, but the paired foramina are never teardrop shaped), and they do not extend posteriorly to the level of M1. The maxillary portion of the septum is comparatively wide (fig. 4B). A median process on the posterior palatal margin may be present or absent. The posterolateral palatal pits are small, shallow, and posterior to M3; usually two or three pits are present on each side of the posterior palatal, but only one pit was found unilaterally in 10 of 75 specimens examined. The auditory bullae are more or less flask shaped, with short and wide bony eustachian tubes. The carotid canal has a small aperture (fig. 11). In frontal view (fig. 5B), the infraorbital foramen is narrow, and the zygomatic plate is slim and delicate.
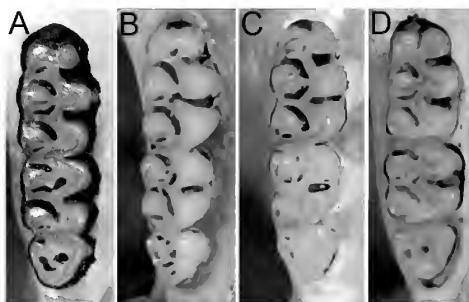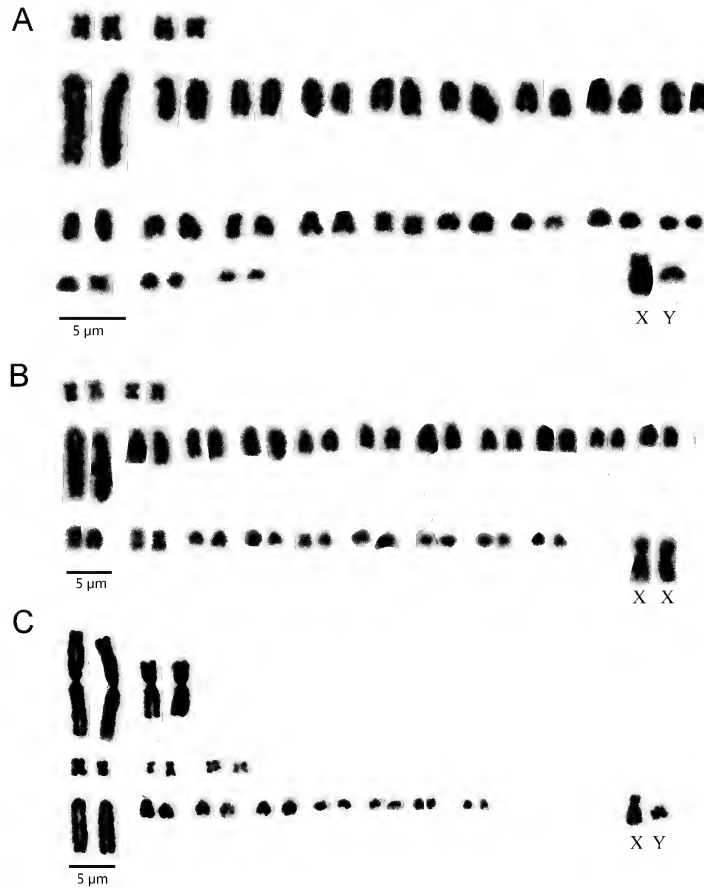
FIGURE 7. Karyotype of male (**A**, MUSM 44963) and female (**B**, MUSM 44964) specimens of *Neacomys rosalindae,* 2n = 48/FN = 50; and of a male specimen of *Neacomys macedoruizi* (**C,** MUSM 45053), $2n = 28/$ FN = 36.

The maxillary toothrow is short in proportion to the diastema. The first upper molar (M1) is oval in occlusal outline, the anterocone is rounded and contains a small internal fossette (fig. 6B, C), and the anteromedian flexus is usually weakly developed (observed mainly in specimens of age classes II and III); the anteroloph is usually fused with the anterocone (fig. 6B) and, in some specimens, it is short (not reaching the labial margin of the tooth), straight, and slender (fig. 6C); the anteroflexus is missing; the mesoloph is narrow but robust, straight, and extends to the labial cingulum; the posteroloph is short and slim; the paraflexus is distinct and large, and the mesoflexus is also distinct but variable in length; the metaflexus is distinct and very long; the posteroflexus is a short internal fossette, whereas the protoflexus and hyploflexus are very distinct. M2 is approximately square in occlusal outline and exhibits a distinct internal fossette; the anteroloph is slender but conspicuous; the mesoloph is slightly curved or straight; the posteroloph is distinct and wide; the paraflexus is distinct and long; the mesoflexus is short; and the metaflexus is very long. M3 is small, almost half the size of M2, and is subtriangular in occlusal out-

FIGURE 8. Hernando de Macedo Ruiz in the exhibition of primates at the Museo de Historia Natural, Lima, Peru on 28 February 2011. Photo by Víctor Pacheco.

line. This molar has a short but distinct anteroloph, a short paraflexus, and the distinct metaflexus is a small fossette.

On the mandible, the anteromedian flexid of m1 is usually absent; the anterolophid is fused with the anteroconid; the mesolophid is poorly developed and usually fused lingually with the entoconid; the posterolophid is also fused with the entoconid; the metaflexid is relatively long and usually in contact with the mesoflexid, which is also very long; the entoflexid is reduced as a small fossette; and the protoflexid and hypoflexid are clearly evident. On m2 the antero-labial cingulum is very slender; the protoflexid is distinct but short and not very deep; the hypoflexid is long and deep; the mesoflexid is long; the mesolophid is usually fused with the entoconid, and the entoflexid is not evident; the posterolophid is wide and fused at the lingual margin of the tooth with the entoconid. On m3 the protoconid, metaconid, and hypoconid are well developed; the protoflexid is very short or not evident; the hypoflexid is well developed; the mesoflexid and posteroflexid are clearly noticed as a small fossetid; the mesolophid and entoconid are fused and not well defined, while the posterolophid is clearly evident.

KARYOTYPES: Conventional cytogenetic preparations were made for three specimens (MUSM 44964, a female; and MUSM 44963 and 44968, both males). The karyotype ($2n = 48$, FN = 50) consists of two pairs of small metacentric autosomes and 21 pairs of acrocentric autosomes (of which one pair is large, 11 are medium, and nine are small); the X chromosome is submetacentric, whereas the Y chromosome is a small acrocentric (figs. 7A, 7B).

FIGURE 9. *Neacomys rosalindae* (MUSM 44971). Photo by Víctor Pacheco.

MEASUREMENTS OF HOLOTYPE: HBL, 99; TaL, 66; HFL, 22; EL, 12.5; CIL, 19.12; ZB, 11.15; BB, 10.04; IOC, 4.01; RL, 6.81; NL, 8.44; RW-1, 3.96; RW-2, 3.24; OL, 7.39; DL, 5.72; MTRL, 2.56; IFL, 2.7; PL, 8.78; AW, 3.93; OCB, 9.33; BOL, 3.07; MPFL, 2.78; MPFW, 1.72; ZPL, 1.92; CD, 7.95; BIF, 1.53; BPB, 2.30; BM1, 0.76. Measurements of additional specimens are provided in table 1.

DISTRIBUTION AND SYMPATRY: Based on specimens examined (appendix 1) and the descriptions by Tirira (2007) and Hice and Velazco (2012), *Neacomys rosalindae* is distributed north of the Amazon River in northeastern Peru (Amazonas and Loreto departments) and eastern Ecuador (Pastaza and Napo provinces), where the species has been reported from different types of lowland primary forest, such as *varillal, monte alto*, and *franco arcilloso* (Álvarez, 1997; García et al., 2003, Hice and Velazco, 2012). *Neacomys rosalindae* occurs sympatrically with *N. amoenus*.

COMPARISONS: *Neacomys rosalindae* could be confused with several other small-bodied species from western Amazonia, including *N. minutus, N. musseri*, and *N. macedoruizi*. In addition, *N. rosalindae* merits comparison with the northwestern South American species *N. tenuipes*, because some Ecuadorian specimens were earlier confused with it (Lawrence, 1941).

Neacomys rosalindae differs from *N. musseri* by its smaller caudal scales (17–24 rows/cm versus 16 rows/cm, on average, in *N. musseri*; Patton et al., 2000); carotid circulation pattern 1 (versus pattern 2 [sensu Voss, 1988]); shallow (versus deep) M1 anteromedian flexus; smaller subquamosal fenestra; shorter incisive foramina; and a karyotype of $2n = 48$, FN = 50 (versus $2n = 34$, FN = 64–68).

Neacomys rosalindae differs from *N. minutus* principally by its more globose skull and shorter rostrum (table 1); gently curved and smoothly divergent (versus straighter and more strongly

FIGURE 10. *Neacomys rosalindae* (MUSM 44971). **A**, Dorsal and ventral views of the skin specimen. **B,** the same specimen showing the white hair bases of the ventral fur.

FIGURE 11. Dorsal, ventral, and lateral views of the cranium and mandible of *Neacomys rosalindae* (MUSM 44963, holotype).

divergent) supraorbital ridges; smaller subsquamosal fenestra and postglenoid foramen; shorter, subrectangular (versus teardrop-shaped) incisive foramina; wider maxillary portion of the septum of incisive foramina; presence of more than one posterolateral palatal pit on each side (versus a single large pit; fig. 4A, B); and a karyotype of $2n = 48$, FN = 50 (versus $2n = 35$–36, FN = 40).

Neacomys rosalindae differs from *N. tenuipes* by its shorter (versus longer) outer toes (Voss et al., 2001: table 19; Weksler and Bonvicino, 2015); relatively longer and less distinctly bicolored tail (tables 1, 2); pure white (versus sometimes buffy or orange) ventral fur; inconsistent presence of an orange lateral line (versus an always-conspicuous orange lateral line); a smaller and globose versus a longer skull (CIL, table 1); an interorbital region with posteriorly divergent lateral margins (versus an hourglass-shaped interorbit); smaller subsquamosal foramen; shorter rostrum (RL, table 1); shorter toothrow (MTR, table 1); an oval (versus rectangular) M1 with a weak (versus a conspicuous) anteromedian flexus; and $2n = 48$ (versus $2n = 56$) chromosomes.

Neacomys rosalindae differs from *N. macedoruizi* by its pure white (versus gray-based) ventral hairs, shorter incisive foramina with a wider maxillary part of the septum, slightly (versus strongly) divergent supraorbital ridges, smaller subsquamosal and postglenoid openings, a narrower infraorbital foramen (fig. 5), rounded (versus straight) outer border of the M1 anterocone, shallow (versus deep) anteromedian flexus on M1, the presence (versus absence) of an internal fossette on the anterocone (fig. 6), and $2n = 48$ (versus $2n = 28$) chromosomes.

Neacomys rosalindae is easily distinguished from its sympatric congener *N. amoenus* by its size (e.g., HBL <80 mm versus HBL >80 mm), smaller hind feet (HF <22mm versus HF >22), smaller caudal scales (17–24 scale rows per cm versus 14–16 scale rows per cm), paler dorsal coloration, shorter maxillary toothrows (MTRL <2.75 mm versus MTRL >3.00 mm), and subrectangular (versus teardrop-shaped) incisive foramina.

REMARKS: *Neacomys* "sp. nov." reported by Hice and Velazco (2012) from the Allpahuayo-Mishana Reserve southwest of Iquitos in the department of Loreto (Peru) agrees with the features of *N. rosalindae*. Similarly, specimens determined as *N. minutus* (MUSM 17605, 17623, 17624, and 17714) by Hurtado and Pacheco (2017) from the Pucacuro River in the department of Loreto are also assigned here to *N. rosalindae*. Additionally, Lawrence (1941: 427) reported two specimens from "Curaray, Ecuador"[4] (AMNH 71539, 71540) as *N. tenuipes* that were subsequently reidentified by Hurtado and Pacheco (2017) as *N. amoenus carceleni*; however, according to our own examination of both specimens, they are, in fact, *N. rosalindae*. Moreover, as will be clarified in the molecular section of this paper, specimens from Yasuní National Park in eastern Ecuador (Napo province) that Patton et al. (2000: table 22) referred to as *N.* "sp. clade 3" are also *N. rosalindae*.

ETYMOLOGY: The species is named in honor of Rosalind Franklin (1920–1958), whose pioneering X-ray diffraction studies of DNA structure were an important milestone of 20th century biology.

---

[4] Lawrence (1941) believed that this Olalla locality, properly known as "Boca Río Curaray," was in Ecuador, but it is actually in Loreto department, Peru (Wiley, 2010).

Molecular Results

Phylogenetic trees obtained with ML and BI strongly support the monophyly of *Neacomys*, which includes 14 highly divergent clades organized in three main groups. Following Hurtado and Pacheco (2017), we refer to the latter as the *paracou*, *spinosus*, and *tenuipes* groups (fig. 12). The new species, *N. macedoruizi* and *N. rosalindae*, were both recovered as members of the *tenuipes* group. Within the *tenuipes* group, the two species described as new in this report form a weakly supported cluster together with two other western Amazonian taxa, *N. minutus* and *N. musseri*. Unfortunately, basal relationships within this western Amazonian complex are not convincingly resolved, although *N. rosalindae* was recovered as the weakly supported sister group to all the others. In addition to Peruvian sequences newly obtained by us, *N. rosalindae* includes several sequences from eastern Ecuador (Yasuni National Park) that Patton et al. (2000) previously referred to "*Neacomys* sp. clade 3." The monophyly of this species is strongly supported and, despite its wide geographic range across eastern Ecuador and northeastern Peru, it exhibits minimal intraspecific divergence (only 0.90%; appendix 3).

By contrast, *Neacomys macedoruizi* was recovered with strong support as belonging to a cluster that includes two haplogroups currently associated with the name *N. minutus*. Although the relationship is not strongly supported (bootstrap value = 56, posterior probability = 88), *N. macedoruizi* appears to be the sister taxon of the so-called upriver clade of *N. minutus* (sensu Patton et al., 2000).[5] Uncorrected pairwise distances among the three haplogroups in this cluster (the upriver and downriver clades of *N. minutus* plus *N. macedoruizi*) are in the range of 4.9%–7.7% (appendix 3).

Morphometric Analyses

Principal components analysis shows a clear morphometric separation between *Neacomys rosalindae* and its closest relative, *N. minutus* (fig. 13A). The first two components together explained 62.72% of the total variance, and PC2 (which accounts for 12.05%) accounts for most of the interspecific separation in this bivariate plot. The variables RL, RW-2, MB, and CD contributed to the differentiation. Not surprisingly, MANOVA found a significant difference between these obviously divergent species ($\lambda = 0.15$, $p < 0.05$).

Less convincingly, PCA shows a tendency of separation between *N. minutus* and *N. macedoruizi*. The axis of species separation is most closely aligned with PC 2 (fig. 13B), on which MB, CB, and BB were the variables that contributed the most. However, MANOVA found no significant difference between these two species, plausibly because of our very small sample for *M. macedoruizi*.

Lastly, PCA suggests that *Neacomys rosalindae* is partially but incompletely separated morphometrically from *N. tenuipes*, the species with which it has sometimes been confused by previous researchers (fig. 13C). In this analysis, PC1 explains 79.45% of the total variance and is strongly correlated with the variables CIL and BB, whereas PC2 explains only 9.44% of the

---

[5] As recovered in our analyses, this "upriver clade" includes a specimen from Jenaro Herrera previously identified erroneously as *N. amoenus carceleni* (MUSM 15995) by Hurtado and Pacheco (2017).
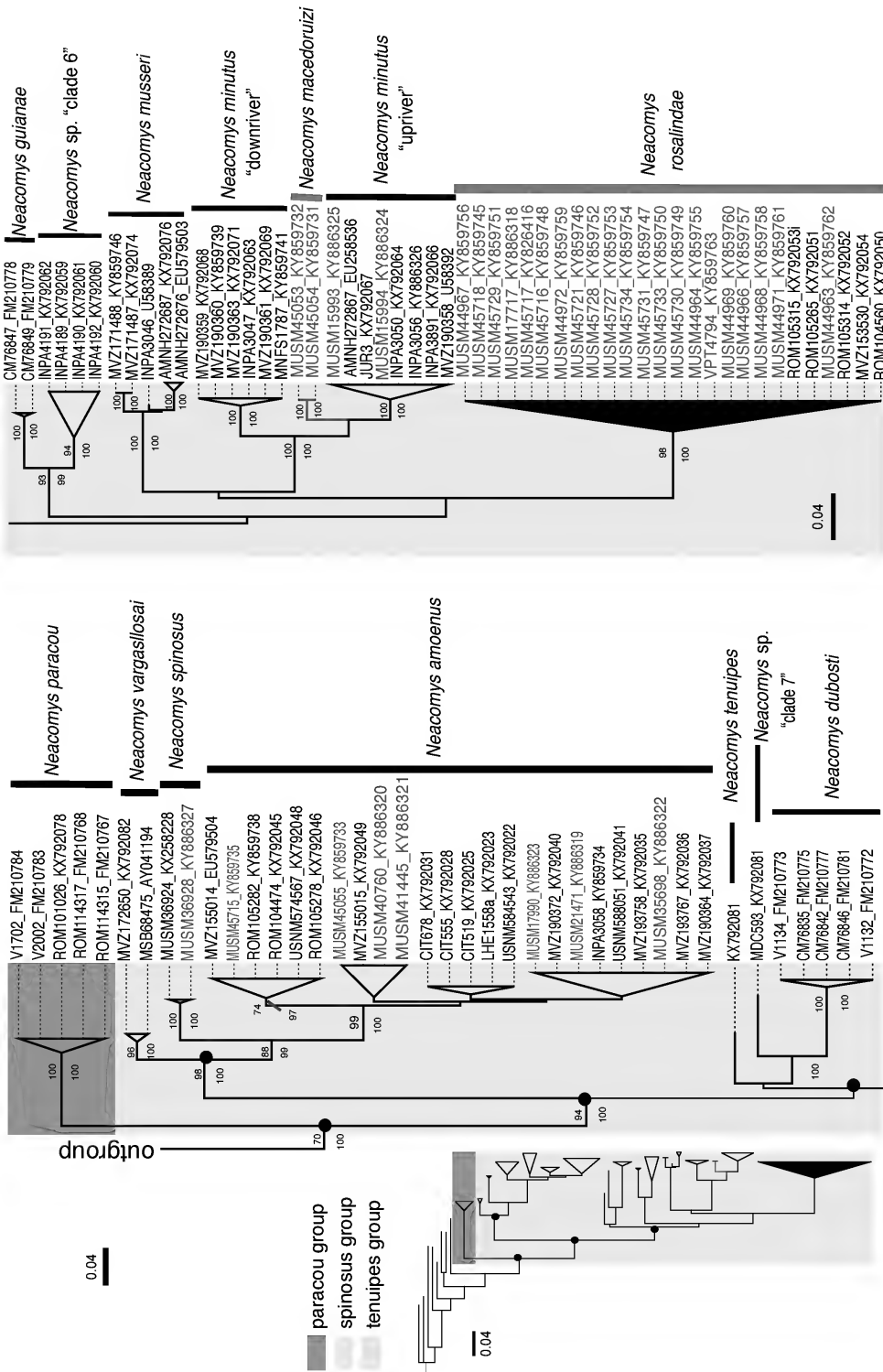
FIGURE 12. Phylogenetic tree of *Neacomys*. Numbers above each branch represent bootstrap values (BS). BS ≥ 90% is considered as strong support, and BS < 70% as lower support. Numbers below each branch represent posterior probabilities (PP). PP ≥ 95% indicate strongly supported nodes. Blue tags refer to cyt-*b* sequences generated in this study.

variance. Also, the MANOVA shows that both species differ significantly ($\lambda = 0.23$, $p <0.05$, fig. 13C). Factor loadings for each analysis are provided in appendix 4.

DISCUSSION

Only two valid species of small-bodied *Neacomys* were previously known from western Amazonia, so the additional species described as new in this report add substantially to the diversity of the genus in this still-incompletely inventoried region. Additionally, the results reported herein have implications for several aspects of the systematics and biogeography of spiny mice, once thought to comprise just three species (Cabrera, 1961), but which may, in fact, be among the most diverse genera of living oryzomyines.

Among other noteworthy results, our phylogenetic analyses corroborate the monophyly of the large-bodied species of *Neacomys* (the *spinosus* group of Hurtado and Pacheco, 2017) as well as the paraphyly of the small-bodied species. The latter conclusion follows from the fact that *N. paracou* (comprising the monotypic *paracou* group), a small-bodied species, is the sister taxon to all other species in the genus. The other small-bodied species, comprising the *tenuipes* group, is the sister taxon of the large-bodied species. Although these groups were also recovered by Hurtado and Pacheco (2017), the *tenuipes* group is only weakly supported in our analyses (as in those by Catzeflis and Tilak, 2009). Therefore, additional studies incorporating more individuals and additional molecular markers are clearly needed to verify the monophyly of the *tenuipes* group and the relationships among the species that belong to it.

Patton et al. (2000) reported that *Neacomys minutus* included two highly divergent haplogroups (informally referred to as the "upriver" and "downriver" clades), and despite highly significant morphometric differences between these haplogroups (based on discriminant analyses), they treated this species as monotypic. However, our molecular analyses, which recovered *N. macedoruizi* as the weakly supported sister taxon of the upriver clade, further support the notion that *N. minutus* (sensu Patton et al., 2000) is, in fact, a species complex. Because the holotype of *N. minutus* belongs to the downriver clade (hereafter, *N. minutus* sensu stricto), it is the upriver clade that currently lacks a name (contra Weksler and Bonvicino, 2015). Although the genetic distances estimated among *N. macedoruizi*, *N. minutus* sensu stricto, and the upriver clade of *N. minutus* are among the lowest yet reported for interspecific comparisons in the genus (4.9%–7.7%; appendix 3), they are still within the range of interspecific distances previously reported among congeneric mammalian species (Bradley and Baker, 2001; Baker and Bradley, 2006), and they are much higher than estimated levels of intraspecific genetic variation (0.5%–3.2%; appendix 3).

Similarly, Patton et al. (2000: 94) suggested that Malygin and Rosmeriak´s specimen (= *Neacomys* sp.) from Jenaro Herrera, Loreto, could be the same as *N.* "sp. (clade 3)," but the karyotype described by Aniskin (1994: fig. 19) of this species clearly shows that is not *N. rosalindae*. On the contrary, the karyotype of Aniskin's unnamed species ($2n = 30$–32 plus 1–6 B
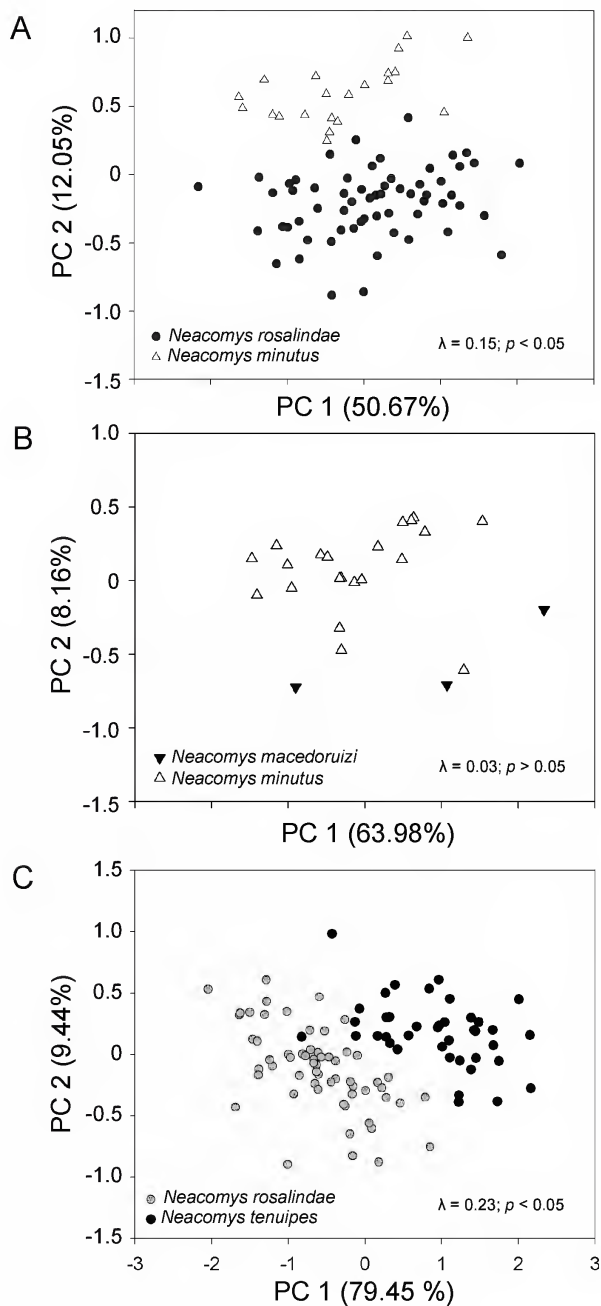
FIGURE 13. Graphical results of principal components analyses. **A,** Comparison between *Neacomys rosalindae* and *N. minutus.* **B,** Comparison between *N. macedoruizi* and *N. minutus.* **C,** Comparison between *N. rosalindae* and *N. tenuipes.* Test statistics in lower-right corner of each panel are from MANOVAs.

TABLE 3. Karyotypes available for species of *Neacomys*. Diploid number (2*n*), fundamental number (FN), autosomal complement classification: Group A (gA) = large-sized metacentric and submetacentric chromosomes, group B (gB) = medium and small sized met or submetacentric chromosomes, group C (gC) = medium and small size subtelocentric chromosomes, group D (gD) = large, medium and small sized of acrocentric chromosomes; and the morphology of sexual chromosomes X and Y. M = metacentric, SM = submetacentric, ST = subtelocentric, A = acrocentric, m = medium size, and s = small size.

Species	2n	FN	gA	gB	gC	gD	X	Y	References
N. paracou	56	62/66	0	12/8	0	42/46	ST	T	da Silva et al. (2015)
N. amoenus[1]	64	68	0	6/6	0	56/56	ST/m, ST	A/s, M	Patton et al. (2000) and Aniskin (1994)
N. tenuipes	56	—	—	—	—	—	—	—	Perez-Zapata et al. (1996)
N. "sp. clade 7"	58	64/70	0	14/8	0	42/48	SM	SM	da Silva et al. (2015)
N. "sp. A"	58	68	0	12	0	44	m, SM	s, SM	da Silva et al. (2017)
N. "sp. B"	54	66	8	6	0	38	m, A	s, A	da Silva et al. (2017)
N. dubosti	62	—	—	—	—	—	—	—	Voss et al. (2001)
N. dubosti	64	68	0	6	0	56	SM	A	da Silva et al. (2015)
N. guianae	56	—	—	—	—	—	—	—	Baker et al. (1983)
N. musseri	34	64/68	2	28	0	4	M or SM	—	Patton et al. (2000)
N. minutus	35-36	40	0	7/6	0	26/28	m-s, M	s, A	Patton et al. (2000)
N. sp.	30-32	38	0	10/9	0	18/21	m, A	s, ST	Aniskin (1994)
N. macedoruizi	28	36	2	8	0	16	m, SM	s, A	Present work
N. rosalindae	48	50	0	4	0	42	m, SM	s, A	Present work

[1] Identified by authors cited in References column as *N. spinosus*, but recent studies confirm that *N. spinosus* is present only in the cloud forest of northern Peru and specimens from lowland forest are in fact *N. amoenus* (Hurtado and Pacheco, 2017).

chromosomes, FN = 38) more closely resembles that of *N. minutus* (2*n* = 35–36, FN = 40; Patton et al., 2000: fig. 75B, C). Both karyotypes are the only ones with three pairs of large acrocentric chromosomes and only one pair of medium-sized submetacentric chromosomes, which also (in both Aniskin's and Patton et al.'s studies) are described with the same heteromorphic states: (1) one submetacentric and two acrocentric chromosomes or (2) two pairs of acrocentric chromosomes. Patton et al. (2000: 110) interpreted this variation as Robertsonian polymorphism, which they observed for specimens of both the upriver and the downriver clades of *N. minutus*. Therefore, it seems likely that Aniskin's and Malygin and Rosmeriak's specimens correspond to the upriver clade of *N. minutus*, an inference that is also supported by our sequencing results.

Crucially, the karyotypes of *Neacomys rosalindae* (2*n* = 48, FN = 50) and *N. macedoruizi* (2*n* = 28, FN = 36) differ strikingly from those of other small-bodied species of *Neacomys* in both chromosome number and morphology. Among other differences, *N. rosalindae* is unique in having only two pairs of small metacentric chromosomes, whereas other species from western Amazonia and those from the Guiana Region have three or more metacentric pairs (table 3; Aniskin, 1994: fig. 19; Patton et al., 2000: fig. 75; da Silva et al., 2015: fig. 2; da Silva et al., 2017: fig. 2,3). Moreover, *N.*

FIGURE 14. Geographic distribution and karyotypes of small-bodied *Neacomys*.

macedoruizi and *N. musseri* are the only small-bodied species that have a single pair of large meta-centrics. Therefore, given the hypothesized role of karyotypic differences as primary isolating mechanisms (White, 1973, 1978; Rieseberg, 2001; Faria and Navarro, 2010) and barriers to introgression (Feder and Nosil, 2009), the divergent karyotype of *N. macedoruizi* provides compelling evidence that it is specifically distinct from the two lineages currently referred to *N. minutus.*

Most species of *Neacomys* retain a large number of acrocentric chromosomes with the same configuration (one large pair and many medium-to-small pairs) and also retain three pairs of small metacentrics (table 3). Based on karyotypic similarities and our phylogenetic results, we agree with da Silva et al. (2015) that the karyotype of *N. paracou* ($2n = 56$, FN = 62/66) could resemble the ancestral karyotype of the genus, particularly since da Silva et al. (2015) found homologies among the acrocentric chromosomes in all species of *Neacomys*. We hypothesize that karyotypic diversification happened independently, at least three times in the genus. Two such events may have resulted in increases of diploid number, once in *N. amoenus*[6] and separately in the clade *N. dubosti* + *N.* "sp. clade 7," both probably due to centric fission (da Silva et al., 2015). A third event probably involved only species from western Amazonia (the *N. minutus* complex, *N. musseri,* and *N. rosalindae*), where a clear reduction of the diploid number is evident (range 28–48), probably the result of Robertsonian changes in *N. macedoruizi* and *N. musseri*. Diploid numbers in *N. tenuipes* and *N. guianae* are similar to that in *N. paracou* ($2n = 56$), but no other comparisons are possible due to the unknown chromosomal morphology of the former two species. Further studies are needed to fill these and other gaps (e.g., the completely unknown karyotype of the Central America species *N. pictus*) and to properly understand karyotypic evolution in *Neacomys*.

The distribution of small-bodied *Neacomys* in Amazonia appears to be bounded mainly by rivers (fig. 14). In western Amazonia, *N. rosalindae* is distributed only north of the Amazon/Marañón (in the Napo region of da Silva et al., 2005), whereas the *N. minutus* complex and *N. musseri* occur south of the Amazon (in the Inambari region; da Silva et al., 2005), suggesting that the upper Amazon is likely an important barrier for these taxa and possibly a driver of speciation. South of the Amazon, *N. macedoruizi* was recorded only on the left bank of the Huallaga, and *N. minutus* and *N. musseri* only on the right bank of the Ucayali River, but faunal sampling is still too sparse in this region to address the possible biogeographic significance of those rivers. More collections of small-bodied *Neacomys* are needed, especially in the Pacaya-Samiria basin—between the Huallaga and Ucayali rivers—to determine which (if any) species of small-bodied *Neacomys* occur there.

ACKNOWLEDGMENTS

---

[6] After the recent revision of the *spinosus* group (Hurtado and Pacheco, 2017), all karyotypes described for *N. spinosus* (e.g., by Gardner and Patton, 1976; Aniskin, 1994; Patton et al., 2000) are now known to correspond to *N. amoenus*. Therefore, the karyotypes for *N. spinosus* and *N. vargasllosai* are still unknown.

REFERENCES

Álvarez, J. 1997. Creación de la Zona Reservada "Allpahuayo-Mishana." Instituto de Investigaciones de la Amazonia Peruana. Iquitos, Perú.

Aniskin, M.V. 1994. Karyological characterization of mammals from the three region of the Republic of Peru. *In* M. Hayka (editor), Mammals of Peruvian Amazonia: 33–47. Moscow: Nauka. [in Russian]

Baker, R.J., and M.B. Qumsiyeh. 1988. Methods in chiropteran mitotic chromosomal studies. *In* T.H. Kunz (editor), Ecological and behavioral methods for the study of bats: 425–435. Washington, DC: Smithsonian Institution Press.

Baker, R.J., B.F. Koop, and M.W. Haiduk. 1983. Resolving systematic relationships with G-bands: a study of five genera of South American cricetine rodents. Systematic Zoology 32: 403–416.

Baker, R.J., M. Hamilton, and D.A. Parish. 2003. Preparation of mammalian karyotypes under field conditions. Occasional Papers of Museum of Texas Tech University 228: 1–8.

Baker, R.J., and R.D. Bradley. 2006. Speciation in mammals and the genetic species concept. Journal of Mammalogy 87: 643–662.

Bradley, R.D., and R.J. Baker. 2001. A test of the genetic species concept: cytochrome *b* sequences and mammals. Journal of Mammalogy 82: 960–973.

Cabrera, A. 1961. Catálogo de los mamíferos de América del Sur. Revista del Museo Argentino de Ciencias Naturales "Bernardino Rivadavia," Ciencias Zoológicas 42: xxii + 309–732.

Catzeflis, F., and M.-K. Tilak. 2009. Molecular systematics of Neotropical spiny mice (*Neacomys:* Sigmodontinae, Rodentia) from the Guiana Region. Mammalia 73: 239–247.

Darriba, D., G.L. Taboada, R. Doallo, and D. Posada. 2012. jModelTest 2: more models, new heuristics and parallel computing. Nature Methods 9: 772.

da Silva, J.M.C., A.B. Rylands, and G.A.B. Fonseca. 2005. O destino das áreas de endemismo. Megadiversidade 1: 124–131.

da Silva, W.O., et al. 2015. Diversity and karyotypic evolution in the genus *Neacomys* (Rodentia, Sigmodontinae). Cytogenetic and Genome Research 146: 296–305.

da Silva, W.O., et al. 2017. Chromosomal diversity and molecular divergence among three undescribed species of *Neacomys* (Rodentia, Sigmodontinae) separated by Amazonian rivers. PLoS ONE 12: 1–19.

Faria, R., and A. Navarro. 2010. Chromosomal speciation revisited: rearranging theory with pieces of evidence. Trends in Ecology and Evolution 25: 660–669.

Feder, J.L, and P. Nosil. 2009. Chromosomal inversions and species differences: when are genes affecting adaptive divergence and reproductive isolation expected to reside within inversions? Evolution. 63: 3061–3075.

Ford, C.E., and J.L. Hamerton. 1956. A colchicine, hypotonic citrate, squash sequence for mammalian chromosomes. Stain Technology 31: 247–251.

García, R., M. Ahuite, and M. Olórtegui. 2003. Clasificación de bosques sobre arena blanca de la zona reservada Allpahuayo-Mishana. Folia Amazónica 14: 17–33.

Gardner, A. L., and J.L. Patton. 1976. Karyotypic variation in oryzomyine rodents (Cricetinae) with comments on chromosomal evolution in the Neotropical cricetine complex. Occasional Papers of the Museum of Zoology, Louisiana State University 49: 1-48.

Goldman, E.A. 1912. Descriptions of 12 new species and subspecies of mammals from Panama. Smithsonian Miscellaneous Collections 56: 1–11.

Hice, C.L., and P.M. Velazco. 2012. The non–volant mammals of the Reserva Nacional Allpahuayo-Mishana, Loreto, Peru. Special Publication Museum of Texas Tech University 60: 1–142.

Hillis, D.M., and J.J. Bull. 1993. An empirical test of bootstrapping as a method for assessing confidence in phylogenetic analysis. Systematic Biology 42: 182–192.

Hurtado, N., and V. Pacheco. 2017. Revision of *Neacomys spinosus* (Thomas, 1882) (Rodentia: Cricetidae) with emphasis on Peruvian populations and the description of a new species. Zootaxa 4242: 401–440.

Lawrence, B. 1941. *Neacomys* from northwestern South America. Journal of Mammalogy 22: 418–427.

Levan, A., F. Karl, and A. Avery. 1964. Nomenclature for centromeric position on chromosomes. Hereditas 52: 201–220.

Malygin, V. M., and M. Rosmiarek. 1996. Morphological difference of two karyotypes of spiny cricentine genus *Neacomys* from Peruvian Amazonia (Rodentia, Mammalian). Doklady Akademii Nauk 351: 712–714.

Patterson, B.D., D.F. Stotz, and S. Solari. 2006. Mammals and birds of the Manu Biosphere Reserve, Peru. Fieldiana Zoology 110: 1–49.

Patton, J.L. 1967. Chromosome studies of certain pocket mice, genus *Perognathus* (Rodentia: Heteromyidae). Journal of Mammalogy 48: 27–37.

Patton, J.L., M.N.F. da Silva, and J.R. Malcolm. 2000. Mammals of the Rio Juruá and the evolutionary and ecological diversification of Amazonia. Bulletin of the American Museum of Natural History 244: 1–306.

Perez-Zapata, A. M. Aguilera, J. Ochoa, and M. Soriano. 1996. Citogenética de roedores de altura: *Microryzomys minutus* y *Neacomys tenuipes*. Acta Científica Venezolana 47: 76.

Reig, O.A. 1977. A proposed unified nomenclature for the enameled components of the molar teeth of the Cricetidae (Rodentia). Journal of Zoology 181: 227–241.

Rengifo, E., and V. Pacheco. 2015. Taxonomic revision of the Andean leaf–eared mouse, *Phyllotis andium* Thomas 1912 (Rodentia: Cricetidae), with the description of a new species. Zootaxa 4018: 349–380.

Rieseberg, L.H. 2001. Chromosomal rearrangements and speciation. Trends in Ecology and Evolution 16: 351–358.

Ronquist, F., and J.P. Huelsenbeck. 2003. MrBayes 3: Bayesian phylogenetic inference under mixed models. Bioinformatics 19: 1572–1574.

Smith, M.F., and J.L. Patton. 1993. The diversification of South America murid rodents: evidence from mitochondrial DNA sequence data for the akodontine tribe. Biological Journal of the Linnean Society 50: 149–177.

Stamatakis, A. 2014. RAxML version 8: a tool for phylogenetic analysis and post-analysis of large phylogenies. Bioinformatics 30: 1312–1313.

Thomas, O. 1882. On a collection of rodents from north Peru. Proceedings of the Zoological Society of London 1882: 98–111.

Thomas, O. 1900. New South American mammals. Annals and Magazine of Nature History (ser. 7) 5: 148–153.

Thomas, O. 1904. On the mammals collected by Mr. A. Robert at Chapada, Matto Grosso (Percy Sladen Expedition to Central Brazil). Proceedings of the Zoological Society of London 1903 (2): 232–244, 1 pl. [usually dated to 1903, but vol. 2 of the 1903 proceedings was published on 1 April 1904]

Thomas, O. 1905. New Neotropical *Chrotopterus*, *Sciurus*, *Neacomys, Coendou, Proechimys*, and *Marmosa*. Annals and Magazine of Natural History (ser. 7) 16: 308–314.

Thompson, J.D., T.J.F. Plewniak, F. Jeanmougin, and D.G. Higgins. 1997. The ClustalX–Windows interface: Flexible strategies for multiple sequence alignment aided by quality analysis tools. Nucleic Acid Research. 25: 4876–4882.

Tirira, D. 2007. Mamíferos del Ecuador. Guía de campo. Publicación especial sobre los mamíferos del Ecuador 6. Quito: Murciélago Blanco.

Voss, R.S. 1988. Systematics and ecology of ichthyomyine rodents (Muroidea): patterns of morphological evolution in a small adaptative radiation. Bulletin of the American Museum of Natural History 188 (2): 259–493.

Voss, R.S. 1991. An introduction to the Neotropical muroid rodent genus *Zygodontomys*. Bulletin of the American Museum of Natural History 210: 1–113.

Voss, R.S., D.P. Lunde, and N.B. Simmons. 2001. The mammals of Paracou, French Guiana: a Neotropical lowland rainforest fauna. Part 2. Nonvolant species. Bulletin of the American Museum of Natural History 263: 1–236.

Weksler, M., and C. Bonvicino. 2015. Genus *Neacomys* Thomas 1900. In J.L. Patton, U.F.J. Pardiñas, and G. D'Elía (editors). Mammals of South America, vol. 2: 339–369. Chicago: Chicago University Press.

White, M.J.D. 1973. Animal cytology and evolution. London: Cambridge University Press.

White, M.J.D. 1978. Modes of speciation. San Francisco: W.H. Freeman.

Wiley, R.H. 2010. Alfonso Olalla and his family: the ornithological exploration of Amazonian Peru. Bulletin of the American Museum of Natural History 343: 1–68.

APPENDIX 1

Neacomys macedoruizi (*N* = 4) — PERU: *Huánuco*, Leoncio Prado, Mariano Damaso Beraún, Tingo María National Park, Puesto de Control 3 de Mayo, road to the "Salto del Ángel" waterfall, 09°24′25.72″ S, 76°0′13.39″ W, 1129 m (MUSM 45053, 45054); Leoncio Prado, Mariano Damaso Beraún, Tingo María National Park, Puesto de Control 3 de Mayo, road to the "Salto del Ángel" waterfall, 09°24′30.29″ S, 76°0′17.69″ W, 943 m (MUSA 19680, 19692)

Neacomys minutus sensu stricto[1] (*N* = 4) — BRAZIL: *Amazonas*, Altamira, right bank Juruá River, 06°35′00″ S, 68°54′00″ W (MVZ 190360, 193061); Barro Vermelho, left bank Juruá River, 06°28′00″ S, 68°46′00″ W (MVZ 190359, 190360).

Neacomys minutus "upriver clade"[2] (*N* = 6) — BRAZIL: *Amazonas,* Penedo, right bank Juruá River, 06°50′0″ S, 70°05′0″ W (MVZ 190358, 190362, 190363). PERU: *Loreto*, Requena, Jenaro Herrera, Centro de Investigación Jenaro Herrera, 04°55′01.2″ S, 73°45′00″ W (MUSM 15993–15995).

Neacomys musseri (*N* = 17) — PERU: *Cuzco,* Paucartambo, Kosñipata, San Pedro, 13°03′16.92″ S, 70°32′46.43″ W, 1480 m (MUSM 19525, 19526). *Loreto,* Ucayali, Contamana, Sierra de Contamana--cerros de Canchaguaya, 07°11′20.11″ S, 74°56′53.7″ W, 320 m (MUSM 17977, 18003); Ucayali, Sierra de Contamana, Aguas Calientes, 07°11′20.11″ S, 74°56′53.7″ W, 230 m (MUSM 18012). *Madre de Dios*, Tahuamanu, 11°11′47.96″ S, 69°46′32.02″ W (MRP 254). *Ucayali,* Purús, Concesión de Conservación Río La Novia, 09°55′47.37″ S, 70°42′07.60″ W, 241–271 m (MUSM 44358–44366, 44567, 44568).

Neacomys rosalindae (*N* = 75) — ECUADOR: *Pastaza*, Mera (USNM 548380). PERU: *Amazonas*, Bagua, Imaza, Comunidad Aguaruna Yamayakat, 05°00′48.7″ S, 78°20′29.04″ W (MUSM 12034–12037, 12039, 12041, 12044); Condorcanqui, El Cenepa, margen derecho de la Quebrada Wee, 03°46′37.60″ S, 78°20′07.91″ W, 690–732 m (MUSM 27061); Condorcanqui, El Cenapa, margen derecho de la Quebrada Wee, 03°38′31.88″ S, 78°18′′36.50″ W, 758 m (MUSM 27063); Condorcanqui, El Cenepa, Huampami, 04°27′24″ S, 78°10′06″ W (MVZ 153530). *Loreto*, Alto Amazonas, Pastaza, Huangana aprox 7.25 km al NW de la boca del Río Pastaza, 04°14′14.89″ S, 76°34′06.60″ W (MUSM 16414–16419); Alto Amazonas, Pastaza, Trueno aprox 2 km al NO de la boca del Río Pastaza, 04°38′52.01″ S, 76°26′59.57″ W (MUSM 16420, 16421); Datem del Marañón, Andoas, Sabaloyacu, 03°31′12″ S, 76°16′12″ W, 180 m (MUSM 25883); Loreto, Tigre, Pucacuro River, 02°42′41″ S, 75°30′01.08″ W (MUSM 17587, 17601, 17604, 17605, 17609–17611, 17623, 17624, 17640, 17643, 17645, 17657, 17658, 17669, 17676, 17679, 17683, 17697, 17703, 17714, 17715, 17717); Loreto, Trompeteros, Nueva Unión, 03°49′01.99″ S, 75°02′55.39″ W, 143 m (MUSM 41136); Loreto, Urarinas, San Antonio de Bancal (6 km to the Urituyacu River's mouth, 04°32′10.28″ S, 75°43′21.32″ W (MUSM 16422, 16423); Maynas, Curaray River, 02°22′0.012″ S, 74°4′59.988″ W (AMNH 71539, 71540); Maynas (MUSM 33871, 33872); Maynas, Punchana, Punto Alegre, 03°28′55.77″ S, 73°25′27.8″ N, 130 m (MUSM 37677); Maynas, San Juan Bautista, 04°08′41.06″ S, 73°27′38.70″ W, 120 m (MUSM 33889); Maynas, San Juan Bautista, Llanchama, 03°52′16.49″ S, 73°23′47.26″ N, 114 m (MUSM 44662); Maynas, San Juan Bautista, Llanchama, 03°52′18.41″ S, 73°23′46″ W, 122 m (MUSM 44963); Maynas, San Juan Bautista, Llanchama near to the Varillal station of the Allpahuayo-Mishana National Reserve, 03°51′57.68″ S, 73°24′38.52″ W, 105 m (MUSM 44964); Maynas, San Juan Bautista, Llanchama near to the Varillal station of the Allpahuayo-Mishana National Reserve, 03°52′28.06″ S, 73°24′10.98″ W, 122 m (MUSM 44965, 44966, 44968); Maynas, San Juan Bautista, Llanchama near to the Varillal station of the Allpahuayo-Mishana National Reserve, 03°52′39.70″ S,

---

[1] The "downriver clade" of Patton et al. (2000).
[2] Of Patton et al. (2000).

73°24′02.02″ W, 126 m; Maynas, San Juan Bautista, km 25 road Iquitos–Nauta, 03°57′34.06″ S, 73°25′18.98″ W, 120 m (MUSM 33873, 33874); Maynas, San Juan Bautista, south bank of the Nanay River, 03°52′41.77″ S, 73°29′08.95″ W, 120 m (MUSM 33892); Maynas, San Juan Bautista, Nina Rumi, 03°51′57.22″ S, 73°23′17.84″ W, 120 m (MUSM 44969–44971); Maynas, San Juan Bautista, Nina Rumi, 03°05′09.36″ S, 73°23′33.04″ W, 106 m (MUSM 44973); Maynas, San Juan Bautista, Nina Rumi, 03°05′09.32″ S, 73°23′35.91″ W, 114 m (MUSM 44972); Maynas, San Juan Bautista, Nuevo Horizonte km 39 road Iquitos–Nauta, 04°04′26.08″ S, 73°27′25.38″ W, 120 m (MUSM 33875); Maynas, San Juan Bautista, Peña Negra km 10 road Iquitos–Nauta, 03°51′13.86″ S, 73°20′48.19″ W, 120 m (MUSM 33895); Maynas, San Juan Bautista, Itaya River, 03°51′17.40″ S, 73°18′24.84″ S, 101 m (MUSM 37678); Maynas, San Juan Bautista, San Gerardo km 18.5 road Iquitos–Nauta, 03°54′24.55″ S, 73°22′02.10″ W, 120 m (MUSM 33934, 33935); Maynas, San Juan Bautista, San Lucas km 44 road Iquitos–Nauta, 04°07′05.99″ S, 73°27′04.61″ W, 120 m (33896–33898); Maynas, San Juan Bautista, Zungarococha, 6.5 km W of the road Iquitos–Nauta, 03°50′02.33″ S, 73°22′37.99″ W, 120 m (MUSM 30350).

Neacomys tenuipes (*N* = 19) — COLOMBIA: *Antioquia*, Valdivia, Quebrada Valdivia, 07°11′0″ N, 75°27′0″ W (FMNH 70119–70121); Zaragoza, 25 km S, 22 km W at La Tirana (USNM 499541, 499546, 499547). *Boyacá*, Muzo, Muzo, 05°31′59.99″ N, 74°06′0″ W (FMNH 71778, 71779). *Caldas*, Samaná, Rio Hondo (FMNH 71751, 71752, 71756). *Cundinamarca*, Paime (AMNH 71347). *Cauca*, Timbique, San José (AMNH 31695). *Huila*, Acevedo, Rio Aguas Claras, 01°37′50.02″ N, 75°59′30.01″ S (FMNH 71768, 71769, 71771, 71772). VENEZUELA: *Falcón*, Serranía de San Luís, JC Falcón National Park (AMNH 276526, 276585)

APPENDIX 2

Specimens Sequenced for Cytochrome *b*

Abbreviations: BMNH, British Museum (Natural History); CM, Carnegie Museum of Natural History mammal collection INPA, Instituo Nacional de Pesquisas da Amazônia; MBUCV, Museo de Biología de la Universidad Central de Venezuela; MN, Museo Nacional, Universidade Federal do Rio de Janeiro; MSB, Museum of Southwestern Biology; ROM, Royal Ontario Museum; other abbreviations are listed in Materials and Methods.

Taxa	Catalog number	Field number	Genbank number	Locality
OUTGROUPS:				
Thomasomys daphne	AMNH 268737	–	DQ914649	Bolivia: La Paz
Rhipidomys macconelli	MBUCV 3306	ALG14059	HM594674	Venezuela: Amazonas
Akodon mollis	FMNH 129212	–	KC841334	Peru: Ancash
Microryzomys minutus	MVZ 173975	–	AF108698	Peru: Cusco
Oligoryzomys microtis	MVZ 193858	–	EU258549	Brazil: Amazonas
Oreoryzomys balneator	AMNH 268144	–	EU579510	Peru: Cajamarca
Oryzomys palustris	–	EVGL 06	EU074639	USA: Florida
Oecomys bicolor	MN37439	–	FJ361049	Brazil: Goiás
INGROUP:				
Neacomys rosalindae	MUSM 45717	PSV 108	KY826416	Peru: Loreto

Taxa	Catalog number	Field number	Genbank number	Locality
Neacomys rosalindae	MUSM 45720	PSV 121	KY859743	Peru: Loreto
Neacomys rosalindae	MUSM 45719	PSV 116	KY859744	Peru: Loreto
Neacomys rosalindae	MUSM 45718	PSV 114	KY859745	Peru: Loreto
Neacomys rosalindae	MUSM 45721	PSV 133	KY859746	Peru: Loreto
Neacomys rosalindae	MUSM 45731	PSV 072	KY859747	Peru: Loreto
Neacomys rosalindae	MUSM 45716	PSV 106	KY859748	Peru: Loreto
Neacomys rosalindae	MUSM 45730	PSV 071	KY859749	Peru: Loreto
Neacomys rosalindae	MUSM 45733	PSV 100	KY859750	Peru: Loreto
Neacomys rosalindae	MUSM 45729	PSV 070	KY859751	Peru: Loreto
Neacomys rosalindae	MUSM 45728	PSV 047	KY859752	Peru: Loreto
Neacomys rosalindae	MUSM 45727	PSV 046	KY859753	Peru: Loreto
Neacomys rosalindae	MUSM 45734	VPT 4475	KY859754	Peru: Loreto
Neacomys rosalindae	MUSM 44964	VPT 4448	KY859755	Peru: Loreto
Neacomys rosalindae	MUSM 44967	KPB 1665	KY859756	Peru: Loreto
Neacomys rosalindae	MUSM 44966	KPB 1661	KY859757	Peru: Loreto
Neacomys rosalindae	MUSM 44968	KPB 1669	KY859758	Peru: Loreto
Neacomys rosalindae	MUSM 44972	KPB 1549	KY859759	Peru: Loreto
Neacomys rosalindae	MUSM 44969	VPT 4396	KY859760	Peru: Loreto
Neacomys rosalindae	MUSM 44971	KPB 1548	KY859761	Peru: Loreto
Neacomys rosalindae	MUSM 44963	KPB 1600	KY859762	Peru: Loreto
Neacomys rosalindae	–	VPT 4794	KY859763	Peru: Loreto
Neacomys rosalindae	MUSM 17717	LAC 538	KY886318	Peru: Loreto
Neacomys rosalindae	MVZ153530	JLP 7102	KX792054	Peru: Amazonas
Neacomys rosalindae	MVZ155299	JLP 7375	KY859730	Peru: Amazonas
Neacomys rosalindae	ROM105314	F 37642	KX792052	Ecuador: Napo
Neacomys rosalindae	ROM104560	F 37413	KX792050	Ecuador: Napo
Neacomys rosalindae	ROM105265	F 37588	KX792051	Ecuador: Napo
Neacomys rosalindae	ROM105315	F 37643	KX792053	Ecuador: Napo
Neacomys macedoruizi	MUSM 45054	PSV 023	KY859731	Peru: Huánuco
Neacomys macedoruizi	MUSM 45053	PSV 021	KY859732	Peru: Huánuco
Neacomys minutus "upriver"	MUSM 15993	JAA 245	KY886325	Peru: Loreto
Neacomys minutus "upriver"	MUSM 15994	JAA 263	KY886324	Peru: Loreto
Neacomys minutus "upriver"	AMNH 272867	RSV 2408	EU258536	Peru: Loreto
Neacomys minutus "upriver"	INPA 3050	JUR 48	KX792064	Brazil: Amazonas
Neacomys minutus "upriver"	–	JUR 3	KX792067	Brazil: Amazonas
Neacomys minutus "upriver"	MVZ 190358	JLP 15365	U58392	Brazil: Amazonas
Neacomys minutus "upriver"	MVZ 190362	MNFS 494	KX792070	Brazil: Amazonas
Neacomys minutus "upriver"	INPA 3891	MNFS 624	KX792066	Brazil: Amazonas
Neacomys minutus "upriver"	INPA 3056	MNFS 642	KY886326	Brazil: Amazonas

Taxa	Catalog number	Field number	Genbank number	Locality
Neacomys minutus s.s.	MVZ 190361	JLP 16061	KX792069	Brazil: Amazonas
Neacomys minutus s.s.	MVZ 190359	JLP 15487	KX792068	Brazil: Amazonas
Neacomys minutus s.s.	INPA 3047	JLP 15486	KX792063	Brazil: Amazonas
Neacomys minutus s.s.	MVZ 190360	JLP 16060	KY859739	Brazil: Amazonas
Neacomys minutus s.s.	–	MNFS 1734	KY859740	Brazil: Amazonas
Neacomys minutus s.s.	MVZ 191209	JLP 16062	KX792072	Brazil: Amazonas
Neacomys minutus s.s.	INPA 3051	MNFS 1735	KX792065	Brazil: Amazonas
Neacomys minutus s.s.	MVZ 190363	MNFS 1718	KX792071	Brazil: Amazonas
Neacomys minutus s.s.	–	MNFS 1787	KY859741	Brazil: Amazonas
Neacomys musseri	INPA 3046	MNFS 1395	U58389	Brazil: Acre
Neacomys musseri	MVZ 171487	JLP 11905	KX792074	Peru: Cusco
Neacomys musseri	MVZ 171488	JLP 11906	KY859742	Peru: Cusco
Neacomys musseri	AMNH 272676	RSV 2049	EU579503	Peru: Loreto
Neacomys musseri	AMNH 272687	RSV 2073	KX792076	Peru: Loreto
Neacomys spinosus	MUSM 36928	PAR 026	KY886327	Peru: Amazonas
Neacomys spinosus	MUSM 36924	CT 716	KX258228	Peru: Amazonas
Neacomys amoenus carceleni	MUSM 45715	PSV 067	KY859735	Peru: Loreto
Neacomys amoenus carceleni	MUSM 45714	PSV 037	KY859736	Peru: Loreto
Neacomys amoenus carceleni	–	PSV 204	KY859737	Peru: Loreto
Neacomys amoenus carceleni	ROM 104474	F 37314	KX792045	Ecuador: Pastaza
Neacomys amoenus carceleni	ROM 105278	F 37603	KX792046	Ecuador: Pastaza
Neacomys amoenus carceleni	ROM 105282	F 37607	KY859738	Ecuador: Pastaza
Neacomys amoenus carceleni	USNM 574567	JFJ 723	KX792048	Ecuador: Pastaza
Neacomys amoenus carceleni	ROM 105290	F 37615	KX792047	Ecuador: Pastaza
Neacomys amoenus carceleni	MVZ 155014	–	EU579504	Peru: Amazonas
Neacomys amoenus "Northern Peru"	MVZ 155015	JLP 7627	KX792049	Peru: Amazonas
Neacomys amoenus "Northern Peru"	MUSM 45055	PSV 020	KY859733	Peru: Huánuco
Neacomys amoenus "Northern Peru"	MUSM 41445	EA 243	KY886321	Peru: Junín
Neacomys amoenus "Northern Peru"	MUSM 40760	MCP 1063	KY886320	Peru: Junín
Neacomys amoenus	MUSM 35698	MCP 750	KY886322	Peru: Junín
Neacomys amoenus	MUSM 17790	JAA 668	KY886323	Peru: Loreto
Neacomys amoenus	MUSM 21471	VPT 3239	KY886319	Peru: Ayacucho
Neacomys amoenus	INPA 3058	MNFS 1262	KY859734	Brazil: Acre
Neacomys amoenus	MVZ 190372	JLP 15674	KX792040	Brazil: Amazonas
Neacomys amoenus	MVZ 190364	JLP 15292	KX792037	Brazil: Amazonas
Neacomys amoenus	MVZ 193767	MNFS 1565	KX792036	Brazil: Acre
Neacomys amoenus	MVZ 193758	MNFS 1236	KX792035	Brazil: Acre
Neacomys amoenus	–	LHE 1558a	KX792023	Bolivia: Santa Cruz
Neacomys amoenus	USNM 584543	LHE 1542	KX792022	Bolivia: Santa Cruz

Taxa	Catalog number	Field number	Genbank number	Locality
Neacomys amoenus	–	CIT 678	KX792031	Brazil: Mato Grosso
Neacomys amoenus	–	CIT 519	KX792025	Brazil: Mato Grosso
Neacomys amoenus	–	CIT 555	KX792028	Brazil: Mato Grosso
Neacomys amoenus	USNM 588051	LHE 1494	KX792041	Brazil: Mato Grosso
Neacomys "sp. clade 6"	INPA 4190	MNFS 2084	KX792061	Brazil: Amazonas
Neacomys "sp. clade 6"	INPA 4191	MNFS 2104	KX792062	Brazil: Amazonas
Neacomys "sp. clade 6"	INPA 4192	MNFS 2023	KX792060	Brazil: Amazonas
Neacomys "sp. clade 6"	INPA 4189	MNFS 2017	KX792059	Brazil: Amazonas
Neacomys dubosti	–	V 1132	FM210772	French Guiana: Saül
Neacomys dubosti	CM 76842	–	FM210777	Surinam: Marowijne
Neacomys dubosti	–	V 1134	FM210773	French Guiana: Saül
Neacomys dubosti	CM 76846	–	FM210781	Surinam: Nickerie
Neacomys dubosti	CM 76835	–	FM210775	Surinam: Marowijne
Neacomys guianae	CM 76847	–	FM210778	Surinam: Nickerie
Neacomys guianae	CM76849	–	FM 210779	Surinam: Saramacca
Neacomys paracou	ROM 101026	F 35024	KX792078	Guyana: Barima–Waini
Neacomys paracou	–	V 1702	FM210784	French Guiana: Nouragues
Neacomys paracou	ROM 114317	F 41347	FM210768	Surinam: Brownsberg Nature Park
Neacomys paracou	ROM 101114	F 35112	KX792079	Guyana: Barima–Waini
Neacomys paracou	–	V 2002	FM210783	French Guiana: Kaw, Camp Caiman
Neacomys paracou	ROM 114315	F 41345	FM210767	Surinam: Brownsberg Nature Park
Neacomys "sp. clade 7"	USNM 549553	MDC 593	KX792080	Brazil: Pará
Neacomys tenuipes	BMNH 1899.10.3.34	–	KX792081	Colombia: Cundinamarca
Neacomys vargasllosai	MVZ 172650	JLP 12979	KX792082	Peru: Puno
Neacomys vargasllosai	MSB 68475	NK25265	AY041194	Bolivia: La Paz

APPENDIX 3

UNCORRECTED PAIRWISE GENETIC DISTANCES AMONG SPECIES OF *NEACOMYS*

Bold diagonal entries indicate intraspecific genetic variation.

	N. rosalindae	N. macedoruizi	N. amoenus	N. spinosus	N. minutus "upriver"	N. minutus s.s.	N. musseri	N. "sp. clade 6"	N. dubosti	N. guianae	N. paracou	N. "sp. clade 7"	N. tenuipes	N. vargasllosai
N. rosalindae	**0.90**													
N. macedoruizi	11.44	—												
N. amoenus	15.33	14.62	**2.56**											
N. spinosus	13.59	14.93	8.67	**0.63**										
N. minutus "upriver"	11.85	4.88	15.81	15.13	**0.81**									
N. minutus s.s.	13.15	5.83	15.56	15.60	7.72	**0.49**								
N. musseri	12.51	14.00	14.99	14.60	14.02	13.10	**2.67**							
N. "sp. clade 6"	13.89	15.06	17.61	15.60	15.42	15.52	15.58	**3.18**						
N. dubosti	13.00	14.19	13.60	15.60	17.16	14.96	14.91	14.09	**0.53**					
N. guianae	12.34	13.24	15.98	16.80	12.84	13.86	14.90	8.91	14.16	**0.50**				
N. paracou	15.44	15.68	15.77	15.22	16.86	16.71	17.57	15.25	16.73	16.74	**1.86**			
N. "sp. clade 7"	13.93	12.25	14.27	16.33	12.96	13.83	14.91	15.42	10.72	13.82	16.28	—		
N. tenuipes	9.35	9.79	12.81	13.67	11.48	13.14	11.79	11.67	15.76	8.77	13.29	13.9	—	
N. vargasllosai	13.38	14.39	9.03	8.20	14.34	14.31	13.15	14.77	14.52	14.88	14.29	13.84	8.69	**1.67**

APPENDIX 4

Factor Loadings for Principal Components Analyses of *Neacomys*

	N. rosalindae vs. *N. minutus*			*N. minutus* vs *N. macedoruizi*			*N. rosalindae* vs. *N. tenuipes*[a]		
	PC1	PC2	PC3	PC1	PC2	PC3	PC1	PC2	PC3
CIL	0.62	-0.08	-0.23	0.59	-0.01	-0.13	0.68	-0.50	0.05
ZB	0.32	0.19	0.23	0.26	0.16	0.24	–	–	–
BB	0.20	-0.01	0.56	0.21	-0.32	0.40	0.56	0.76	-0.17
IOC	0.09	0.06	0.26	0.05	-0.05	0.31	0.15	0.17	0.00
RL	0.24	0.47	-0.06	0.31	0.33	0.21	0.30	-0.22	-0.17
NL	0.34	-0.15	-0.27	0.37	0.25	-0.41	–	–	–
RW-1	0.13	0.11	0.13	0.16	-0.18	-0.21	–	–	–
RW-2	0.04	0.46	0.30	0.03	0.23	0.21	–	–	–
OL	0.23	0.04	-0.10	0.19	0.13	0.25	–	–	–
DL	0.21	0.05	-0.16	0.17	0.10	-0.09	0.24	-0.27	-0.10
MTRL	0.01	0.00	0.06	0.00	-0.07	0.10	0.09	0.12	0.03
IFL	0.04	0.08	-0.04	0.03	0.06	-0.16	0.16	0.08	0.95
PL	0.26	-0.02	-0.23	0.25	-0.01	-0.15	–	–	–
AW	0.10	0.24	0.10	0.08	0.25	0.38	–	–	–
OCB	0.13	-0.05	0.16	0.18	-0.35	0.21	–	–	–
MB	0.23	-0.41	0.28	0.29	-0.46	-0.08	–	–	–
BOL	0.11	-0.01	0.00	0.14	-0.05	-0.11	–	–	–
MPFL	0.08	-0.08	-0.12	0.01	0.13	-0.07	–	–	–
MPFW	0.01	0.25	0.02	0.02	0.27	0.02	–	–	–
ZPL	0.07	0.07	0.02	0.05	-0.01	0.18	0.10	-0.07	-0.20
CD	0.11	-0.43	0.33	0.03	-0.29	0.05	–	–	–
% Variance	50.67	12.05	6.33	63.98	8.16	5.66	79.45	9.44	3.38

[a] Based on a reduced dataset, comprising just the eight craniodental dimensions measured for this study and by Voss et al. (2001), who provided the morphometric data for *Neacomys tenuipes*.